



Chipsmall Limited consists of a professional team with an average of over 10 year of expertise in the distribution of electronic components. Based in Hongkong, we have already established firm and mutual-benefit business relationships with customers from,Europe,America and south Asia,supplying obsolete and hard-to-find components to meet their specific needs.

With the principle of “Quality Parts,Customers Priority,Honest Operation,and Considerate Service”,our business mainly focus on the distribution of electronic components. Line cards we deal with include Microchip,ALPS,ROHM,Xilinx,Pulse,ON,Everlight and Freescale. Main products comprise IC,Modules,Potentiometer,IC Socket,Relay,Connector.Our parts cover such applications as commercial,industrial, and automotives areas.

We are looking forward to setting up business relationship with you and hope to provide you with the best service and solution. Let us make a better world for our industry!



## Contact us

Tel: +86-755-8981 8866 Fax: +86-755-8427 6832

Email & Skype: info@chipsmall.com Web: www.chipsmall.com

Address: A1208, Overseas Decoration Building, #122 Zhenhua RD., Futian, Shenzhen, China



# 45 W adapter demo board

## Using the new 800 V CoolMOS™ P7 and ICE2QS03G quasi-resonant PWM controller

**Authors:** Jared Huntington  
Stefan Preimel

### Scope and purpose

The demo board described in this application note provides a test platform for the new 800 V CoolMOS™ P7 series of high voltage MOSFETs. The adapter uses ICE2QS03G, a second generation current mode control quasi-resonant flyback controller and an IPA80R450P7 800 V CoolMOS™ P7 series power MOSFET. This application note is intended for those that have experience with flyback converter designs and will not go in depth about the overall design process for flyback converters, but will cover specific design aspects for this controller and 800 V CoolMOS™ P7 in charger and adapter applications. It will also look at the overall benefits that the 800 V CoolMOS™ P7 presents for switch mode power supplies. For a detailed introduction on flyback converter design please read [Design guide for QR Flyback converter](#) [1].

### Intended audience

Power supply design engineers

### Table of contents

1	<b>Description</b> .....	2
2	<b>Quasi-resonant flyback overview</b> .....	3
3	<b>ICE2QS03G functional overview</b> .....	4
4	<b>800 V CoolMOS™ P7 overview</b> .....	5
4.1	FullPAK vs. DPAK thermal performance.....	7
5	<b>Design considerations</b> .....	9
5.1	800 V MOSFET.....	9
5.2	UVLO circuit.....	10
6	<b>Demo board overview</b> .....	12
6.1	Demo board pictures.....	12
6.2	Demo board specifications.....	12
6.3	Demo board features.....	13
6.4	Schematic.....	14
6.5	BOM with Infineon components in bold.....	15
6.6	PCB layout.....	16
6.7	Transformer construction.....	17
7	<b>Measurements</b> .....	19
7.1	Test measurements under different line and load conditions.....	19
7.2	Normal operation.....	20
7.3	Surge testing.....	22
7.4	Thermal performance under typical operating conditions.....	23
8	<b>Conclusion</b> .....	26
9	<b>References</b> .....	27

Description

### 1 Description

This 45 W adapter demo board is intended to be a form, fit and function test platform for charger and adapter applications to show the operation of the 800 V CoolMOS™ P7 as well as the overall controller design. The demo board is designed around a quasi-resonant flyback topology for improved switching losses which allows higher power density designs and lower radiated and conducted emissions. A 45 W universal input isolated flyback demo board with a 19 V output based on the ICE2QS03G controller and the P7 MOSFET is described in this application note and test results are presented.

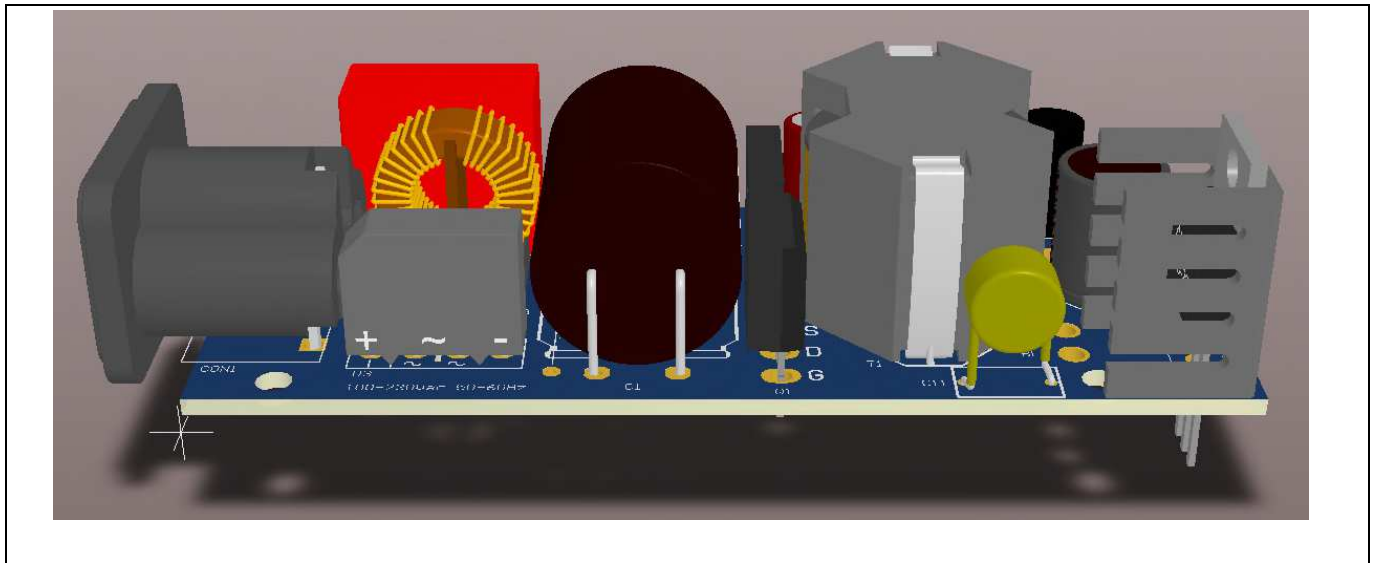


Figure 1 45 W flyback demo board

## 2 Quasi-resonant flyback overview

The QR flyback offers improved efficiency and EMI performance over the traditional fixed frequency flyback converter by reducing switching losses. This is accomplished by controlling the turn on time of the primary MOSFET ( $Q_{pri}$  in Figure 3). In a flyback operating in discontinuous conduction mode (DCM) the energy is first stored in the primary side when the primary MOSFET  $Q_{pri}$  is turned on allowing the primary current to ramp up. The primary MOSFET ( $Q_{pri}$ ) turns off and then the energy stored in the transformer transfers into the secondary side capacitor. The energy that is left in the primary inductance ( $L_{pri}$ ) after transferring the energy to the secondary then resonates with the combined output capacitance of the MOSFET ( $C_{DS\_parasitic}$ ) consisting of the MOSFET output capacitance ( $C_{OSS}$ ), stray drain source capacitance from the transformer and layout, and any additional added external drain source capacitance on this node. In a fixed frequency flyback the switch turn on happens regardless of the  $V_{DS}$  voltage from the MOSFET drain to source. If switching occurs at a higher  $V_{DS}$  (Figure 2) this corresponds to more switching losses ( $E_{OSS}$  losses). The QR flyback waits to turn on  $Q_{pri}$  until the  $V_{DS}$  voltage reaches the minimum possible voltage shown in Figure 2 and then turns on the MOSFET.

$$P_{sw\_on} = 0.5f_{sw}C_{OSS}V_{DS}^2$$

Since the turn on switching losses are a function of  $V^2$  (as shown above), this drastically reduces the overall system switching losses. This has the added benefit of lowering the amount of switched energy which helps reduce switching noise from the converter, resulting in lower radiated and conducted emissions.

800 V CoolMOS™ P7 technology helps improve performance in a QR flyback by allowing an increase in the reflected voltage. This increase in reflected voltage increases the energy stored in the magnetizing inductance during the DCM period which allows switching at an even lower  $V_{DS}$  voltage allowing even lower switching losses. The 800 V CoolMOS™ P7 also has a lower gate charge ( $Q_G$ ) and output capacitance ( $C_{OSS}$ ) which help to further reduce the switching losses of the MOSFET.

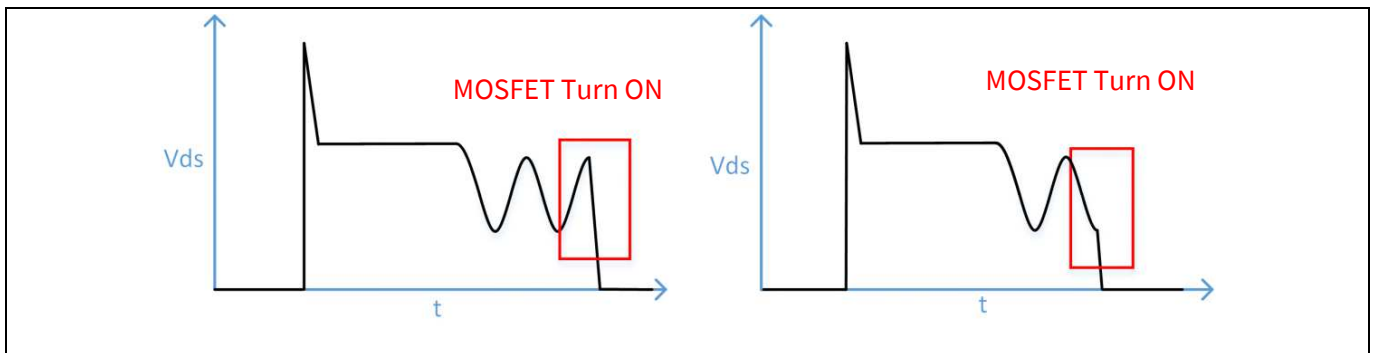


Figure 2 Fixed frequency flyback primary MOSFET drain source waveform (left) vs. a quasi-resonant flyback primary MOSFET drain source waveform (right).

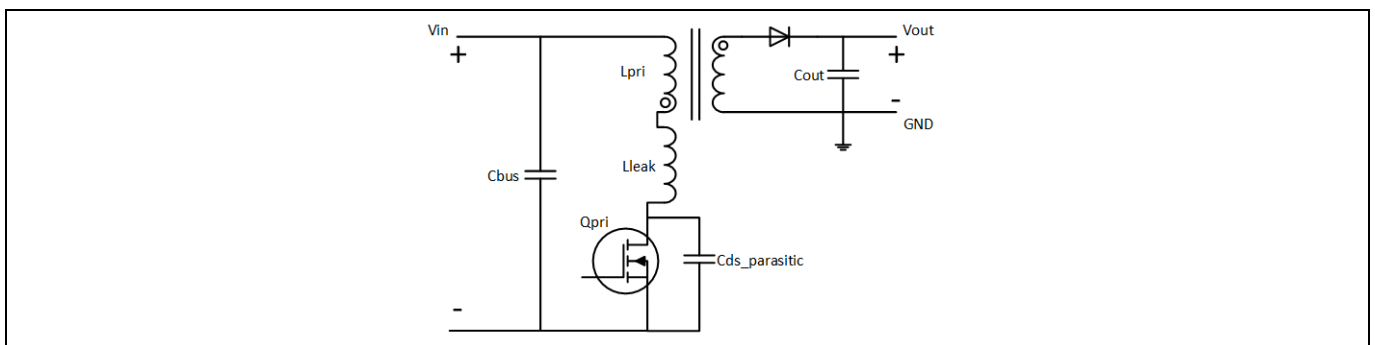


Figure 3 Simplified flyback schematic

### 3 ICE2QS03G functional overview

The PWM controller ICE2QS03G is a second generation quasi-resonant flyback controller IC developed by Infineon Technologies. The typical applications include TV-sets, DVD-players, set-top boxes, netbook adapters, home audio, and printer applications. This controller implements switching at the lowest ringing voltage and also includes pulse skipping at light loads for maximum efficiency across a wide range of loads.

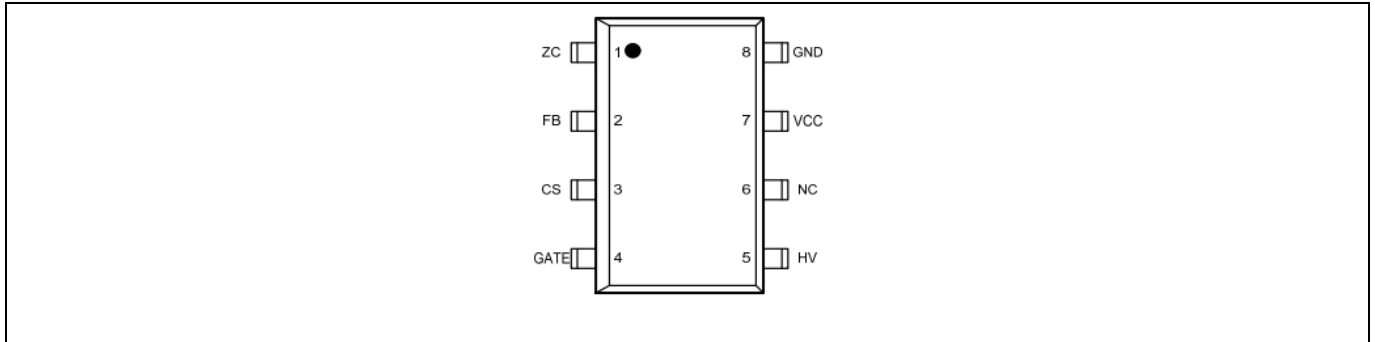


Figure 4 ICE2QS03G pinout

Table 1 ICE2QS03G pin description

Pin	Name	Description
1	Zero Crossing (ZC)	Detects the minimum trough (valley) voltage for turn on for the primary switch turn on time
2	Feedback (FB)	Voltage feedback for output regulation
3	Current Sense (CS)	Primary side current sense for short circuit protection and current mode control
4	Gate drive output (GATE)	MOSFET gate driver pin
5	High Voltage (HV)	Connects to the bus voltage for the initial startup through the high voltage startup cell
6	No Connect (NC)	No connection
7	Power supply (VCC)	Positive IC for the power supply
8	Ground (GND)	Controller ground

## 4 800 V CoolMOS™ P7 overview

The 800 V P7 family of MOSFETs provides several advantages for flyback converters. The 800 V CoolMOS™ P7 offers a cost reduction for the same  $R_{DS(on)}$  device when compared to the C3 series with an improvement in performance. The switching losses of the devices are lowered due to reduced device parasitic elements such as  $C_{OSS}$  and  $Q_G$ . These improvements diminish as the MOSFET drain source voltage during turn on gets lower. The greatest reduction in switching losses is seen at higher drain source switching voltages and at low output powers due to the improved output parasitic elements ( $C_{OSS}$ ). The reduction in overall switching losses of the device allows moving to a higher  $R_{DS(on)}$  to further reduce the BOM cost or allow increasing the power density of the power supply design.

PSpice models of the P7 800 V MOSFETs are provided on the Infineon website. These models have been fitted with measurements of the devices and provide a high level of accuracy. Below, Figure 5 shows the difference between the Infineon 45 W adapter measured waveforms and the simulated waveforms. These models can be used to better understand the loss mechanisms that are responsible for power dissipation in the primary MOSFET of the flyback converter and help optimize designs.

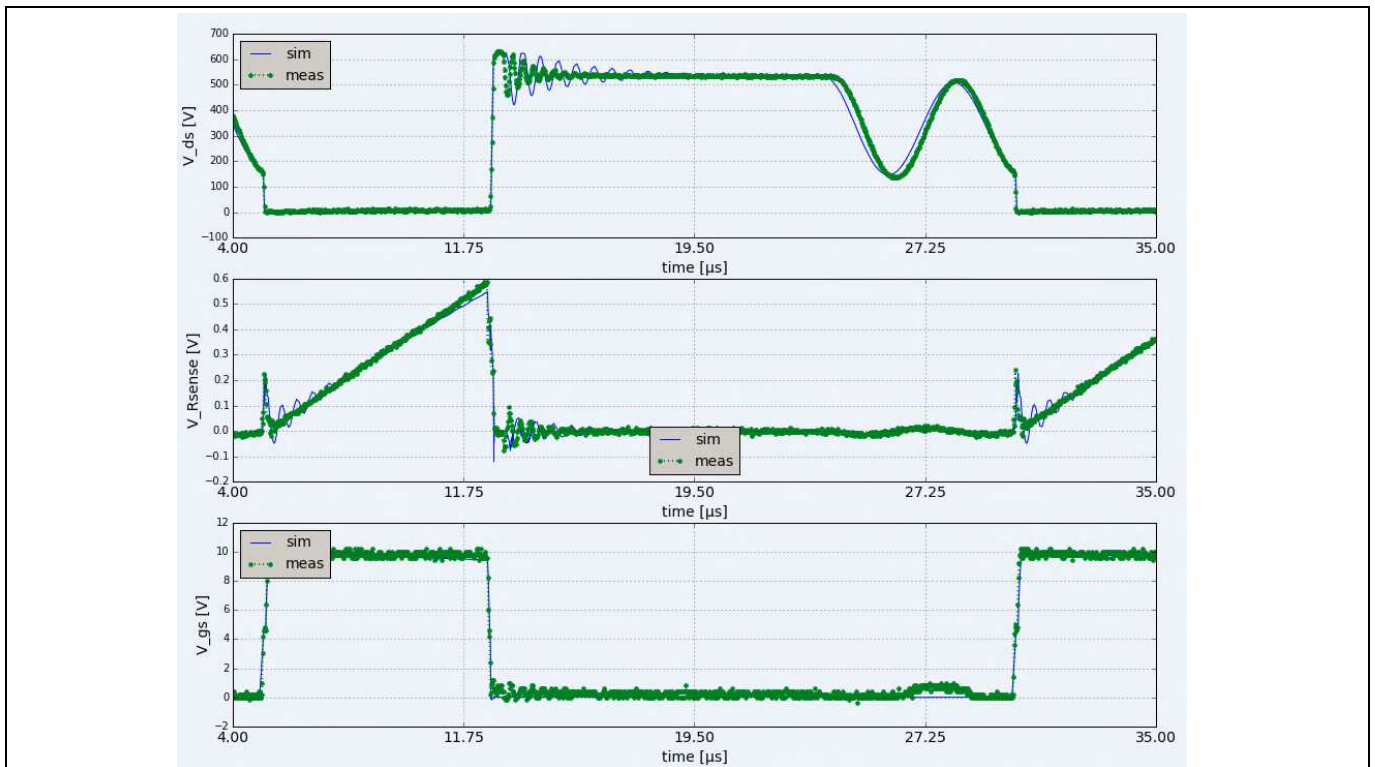


Figure 5 Simulated switching vs. measured switching at 230 V<sub>AC</sub> operation.

# 45 W adapter demo board

## Using the new 800 V CoolMOS™ P7 and ICE2QS03G quasi-resonant PWM controller



### 800 V CoolMOS™ P7 overview

Using the P7 PSpice models for the 45 W adapter, we can look at the losses occurring in the MOSFET of the 45 W adapter flyback converter. The figure below shows the breakdown of the MOSFET turn on losses, turn off losses, and conduction losses. As shown in Figure 6, the switching losses of the MOSFET are a more significant loss contributor at high line. The figure below shows the breakdown of MOSFET turn on losses, turn off losses, and conduction losses at high line. At low line the conduction losses ( $R_{DS(ON)}$ ) dominate and the improvement in  $C_{OSS}$  does not make such a large improvement. The IPA80R1K4P7 MOSFET offers lower switching losses which give a total power savings of 15.6 mW at high line over the original C3 series SPA06N80C3 - with a large reduction in cost.

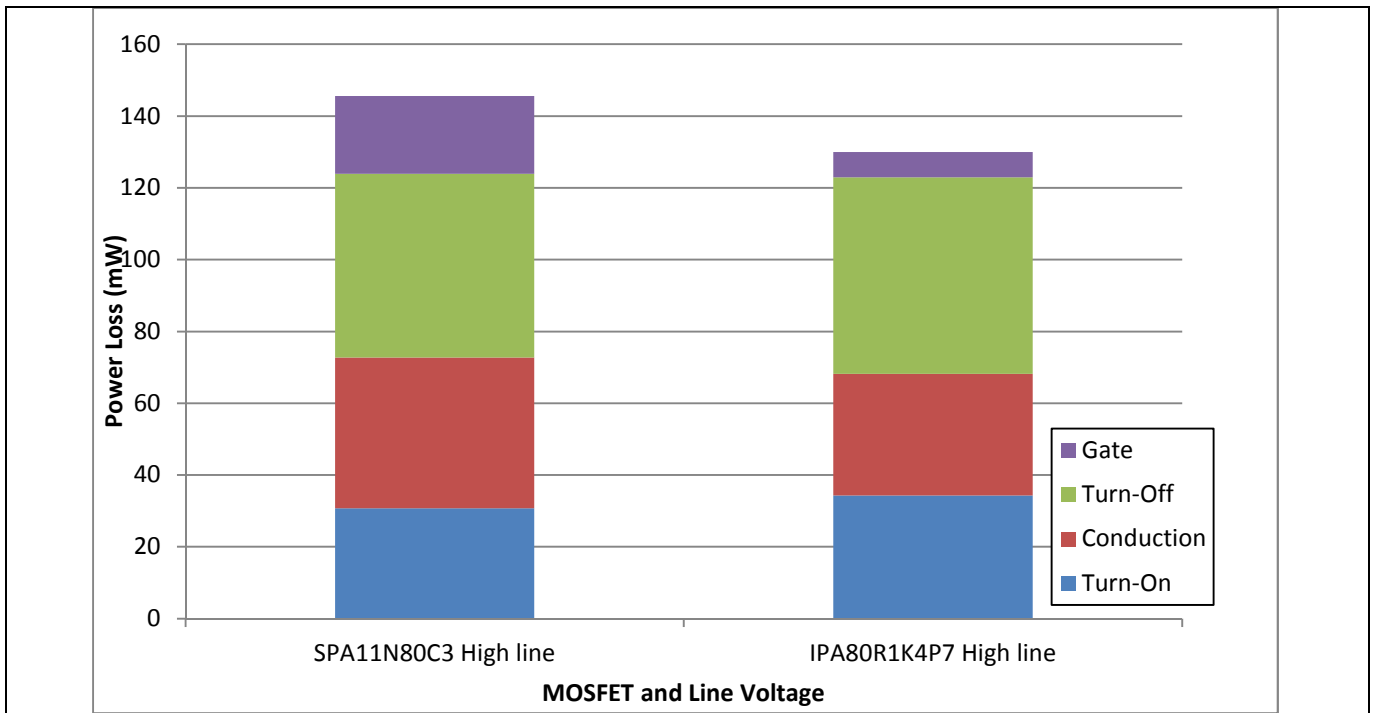


Figure 6 Switching losses of SPA11N80C3 vs. IPA80R450P7 at 230 V<sub>AC</sub> input

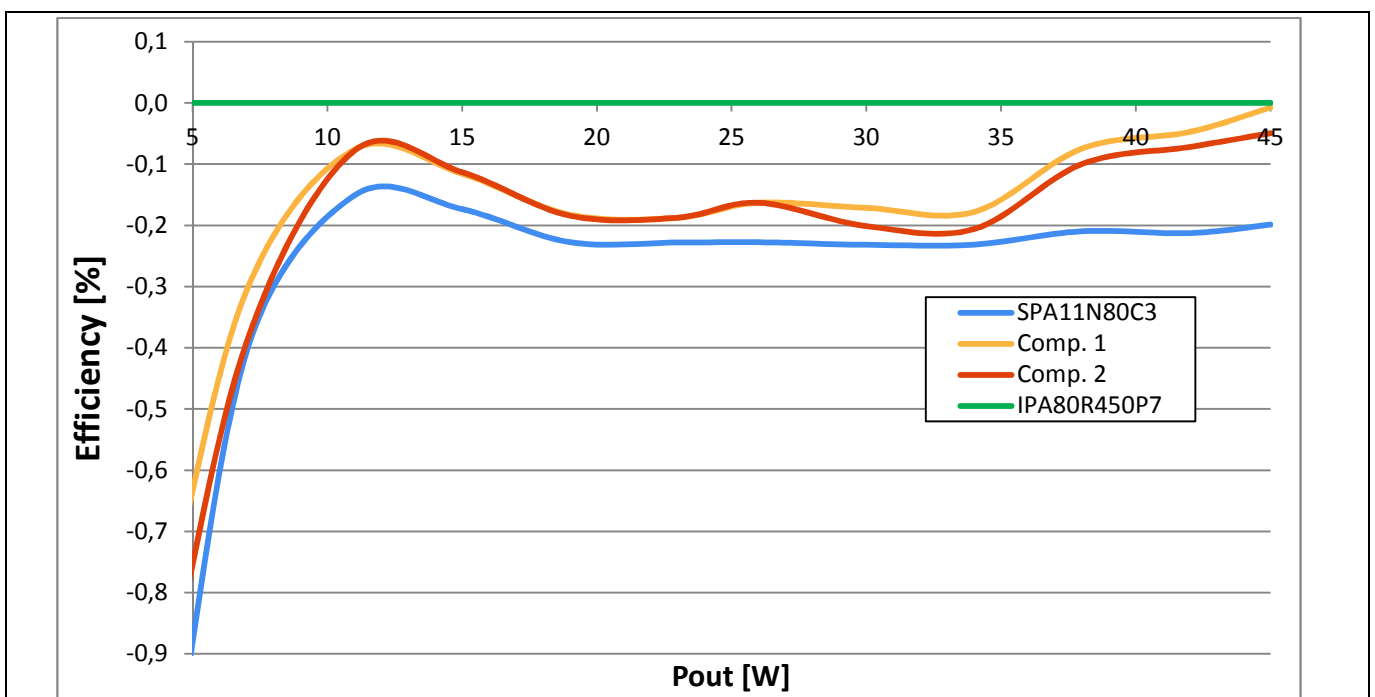


Figure 7 IPA80R450P7 set as the efficiency reference measured in the 45 W adapter in comparison with the SPA11N80C3 and a competitor's equivalent component at 230 V<sub>AC</sub>.

### 800 V CoolMOS™ P7 overview

It can be seen in Figure 7 that the IPA80R450P7 has improved performance when compared to the C3 series of MOSFETs and two of our competitors latest generation of MOSFETs. At light loads the switching losses are dominant and it can be seen that the P7 switching performance is much better.

\*Simulations and modeling done by Stefano De Filippis

## 4.1 FullPAK vs. DPAK thermal performance

The DPAK MOSFET package is ideal for low cost applications such as charger and adapters. The thermal performance is slightly lower than the TO-220 FullPAK (TO-220FP), but it has a lower package cost allowing for overall BOM savings. The DPAK also has a smaller form factor allowing for higher power density designs and the SMD placement to be used. In the Infineon 45 W adapter allows a TO-220FP or a DPAK footprint. The two packages were tested on the same board under full load (45 W) at 120 V<sub>AC</sub> and 230 V<sub>AC</sub> in a 25°C ambient to show the thermal performance difference between the two packages.

**Table 2 FullPAK vs. DPAK thermal performance (25°C ambient)**

Test conditions	IPD80R450P7 DPAK case temp. rise(°C)	IPA80R450P7 FullPAK case temp. rise(°C)	DPAK temp. increase from FullPAK(°C)
45 W, 120 V <sub>AC</sub> , 60 Hz,	56.8°C	27.7°C	29.1°C
45 W, 230 V <sub>AC</sub> , 50 Hz	51.8°C	25.9°C	25.9°C

In the infrared thermal images below, the primary MOSFET Q1 is called out in the black boxes. It can be seen that the temperature of the DPAK is 29.1°C higher than the FullPAK at 120 V<sub>AC</sub>. Most of this temperature difference is due to the fact that the MOSFET (when placed on the bottom side of the printed circuit board) receives some heating from the surrounding components (the snubber and transformer). Figure 10 shows the DPAK footprint temperature rise while the power supply is operating using the FullPAK. This increases the package temperature in addition to the difference in package thermal resistance leading to a higher temperature. The hottest components on the board are the snubber network resistors, R22 and R23, shown below in Figure 8. Table 3 takes the DPAK thermal rise and removes the PCB temperature rise of the footprint with the FullPAK in place. The DPAK temperature is then overcorrected due to some heating of the PCB from the FullPAK causing a higher footprint temperature.

**Table 3 FullPAK vs. DPAK thermal performance normalized for PCB rise (25 °C ambient)**

Test conditions	IPD80R450P7 DPAK case temp. rise(°C)	IPD80R450P7 DPAK footprint temp. rise(°C)	DPAK case temp. increase from PCB temp. (°C)	DPAK temp. increase from FullPAK (°C)
45 W, 120 V <sub>AC</sub> , 60 Hz	56.8°C	30.1°C	26.7°C	-1.0°C
45 W, 230 V <sub>AC</sub> , 50 Hz	51.8°C	29.5°C	22.3°C	-3.6°C

A 50°C ambient would push the total DPAK temperature up to 106.8°C in this specific design. Depending on the required ambient operating conditions the DPAK package in this application would require a larger copper area or lower output power in order to have enough thermal margins under worst case conditions.

The DPAK package can be used to give space, cost, and assembly savings, but the additional heating of surrounding components and reduced thermal performance needs to be considered when switching from a FullPAK to a DPAK package.



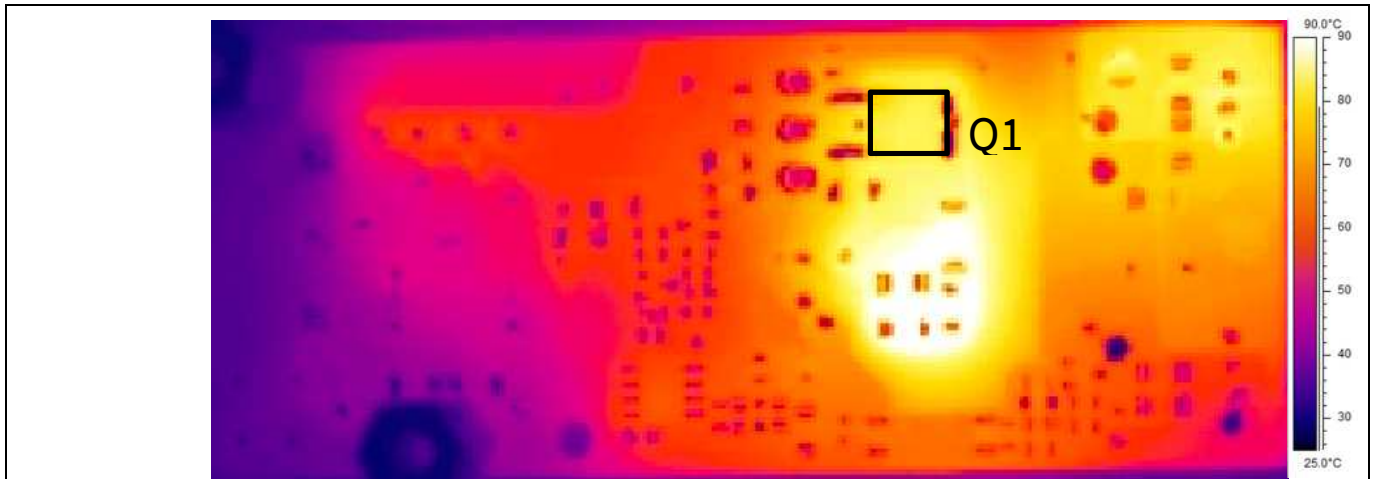


Figure 8 45 W adapter bottom using DPAK at 45 W load and 120 V<sub>AC</sub>. Q1 shown above in the black box is the flyback converter primary MOSFET. Note the MOSFET Q1 is receiving some heating from the surrounding components which contributes to the higher DPAK temperature.

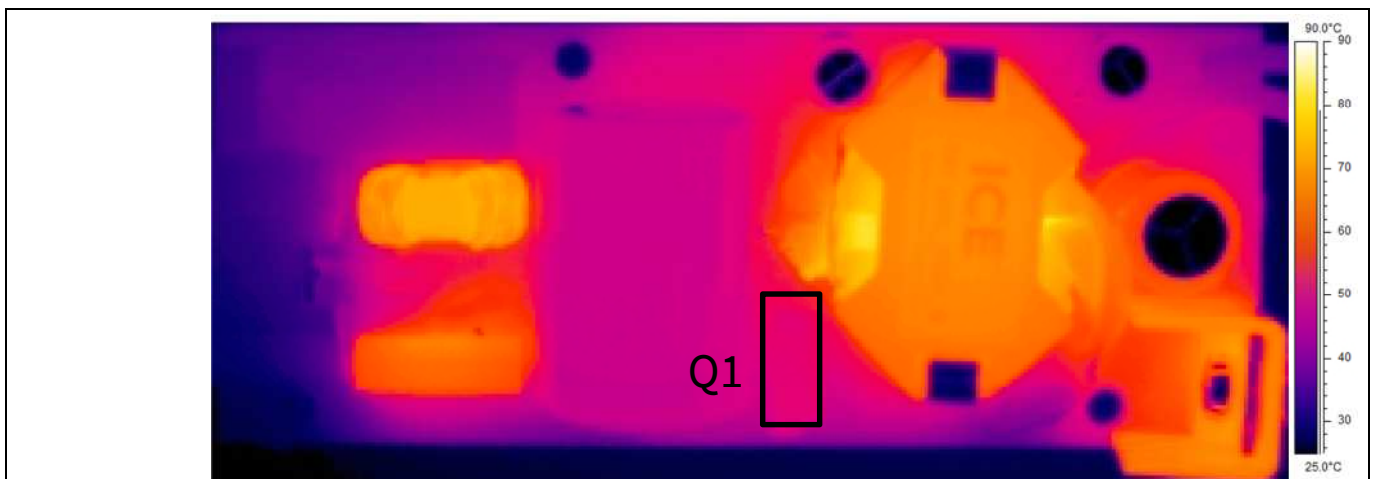


Figure 9 45 W adapter top using FullPAK at 45 W load and 120 V<sub>AC</sub>. Q1 shown above in the black box is the flyback converter primary MOSFET.

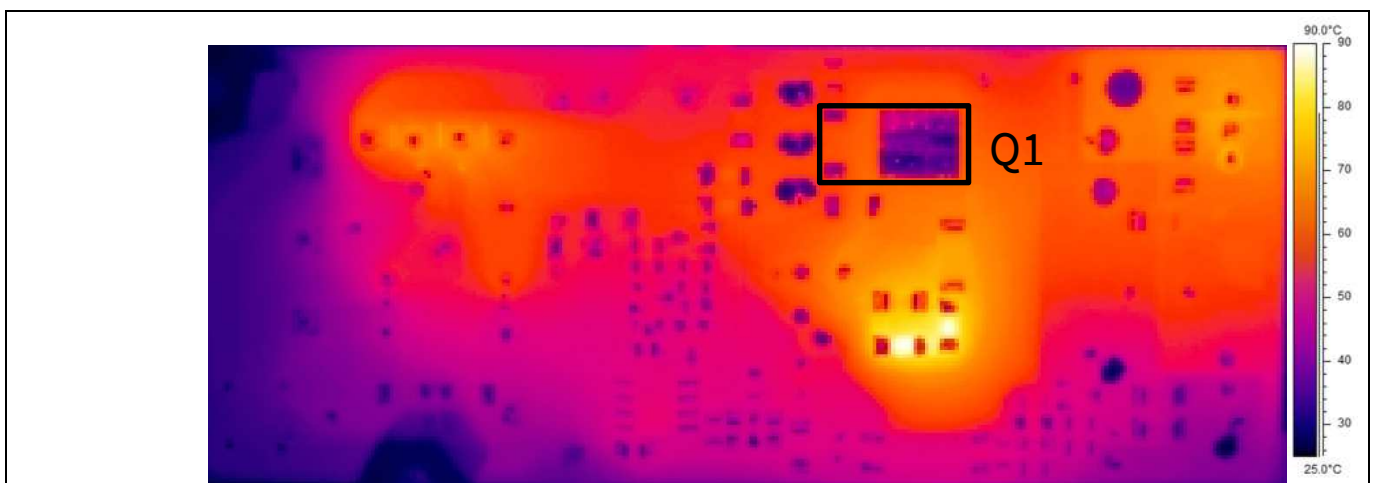


Figure 10 45 W adapter bottom using FullPAK at 45 W load and 100 V<sub>AC</sub>. The DPAK footprint is shown and the local PCB temperature rise can be seen which further increases the DPAK temperature.

## 5 Design considerations

### 5.1 800 V MOSFET

The 800 V CoolMOS™ P7 provides several benefits for charger and adapter applications. An 800 V breakdown voltage allows a higher combination of bus voltage, reflected voltage, and snubber voltage than can be achieved with a 600 V or 650 V device. By allowing a higher reflected voltage and snubber voltage the system power losses can be reduced while maintaining higher breakdown voltage margins.

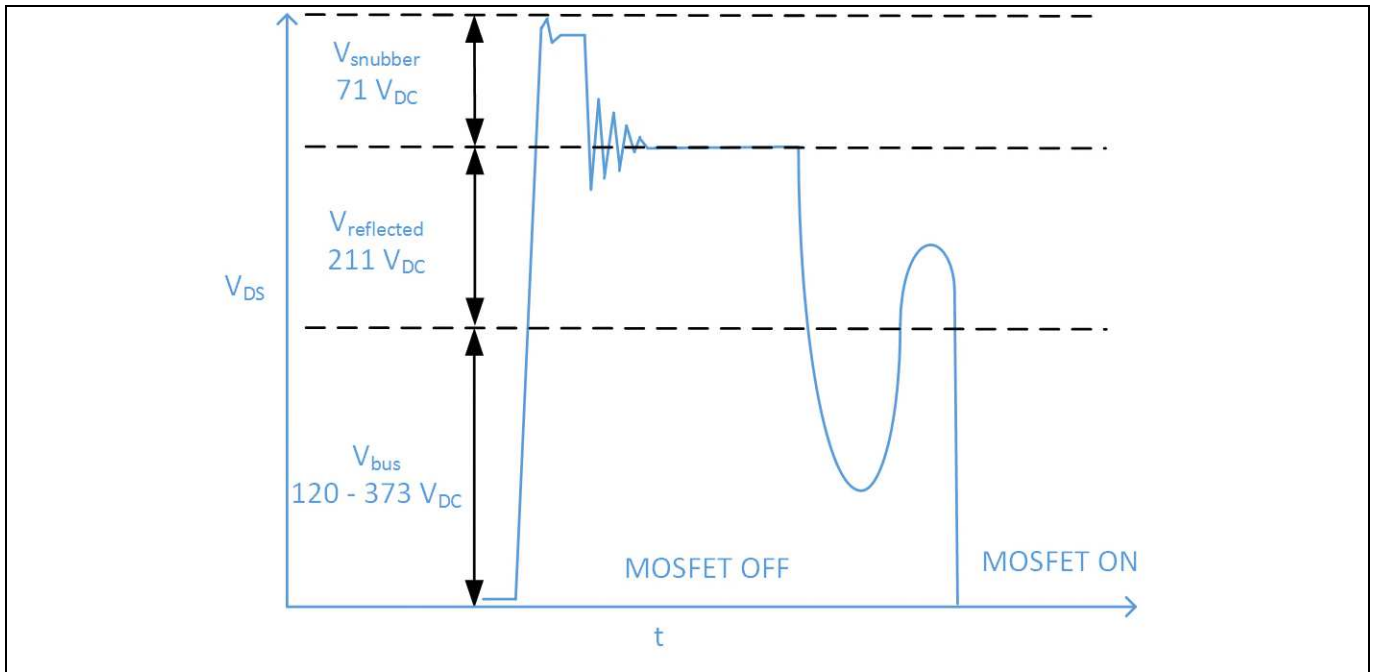


Figure 11 MOSFET  $V_{DS}$  during turn off in the Infineon 45 W adapter

In this specific design the reflected voltage was increased from the Infineon 35 W adaptor which used a 600 V device. This section will compare the Infineon 35 W adapter design using a 600 V MOSFET with the Infineon 45 W adapter using an 800 V MOSFET to show the difference in performance between the two designs.

The reflected voltage determines the trough (valley) voltage during DCM ringing where the switch turns on in the QR flyback converter. By allowing a higher reflected voltage there is a resulting lower trough in the ringing waveform. This allows the converter to switch at a lower  $V_{DS}$  voltage and reduce the system's switching losses especially at high line (265  $V_{AC}$ ) operation.

$$P_{sw\_on} = 0.5f_{sw}C_{DS\_parasitic}V_{DS}^2$$

$$V_{reflected} = \frac{N_P}{N_S}(V_{output} + V_{forward})$$

Table 4

Parameter	Symbol	600 V design	800 V P7 design
Transformer primary turns	$N_P$	66 turns	87 turns
Transformer secondary turns	$N_S$	11 turns	8 turns
Output voltage	$V_{output}$	19 V	19 V
Diode forward voltage	$V_{forward}$	0.55 V	0.4 V
Transformer reflected voltage	$V_{reflected}$	117 V	211 V

### Design considerations

The primary side resistor, capacitor, and diode (RCD) snubber network resistor power dissipation was reduced allowing the snubber voltage to reach a higher level and lowering the amount of energy that is dissipated in the snubber resistor. This especially comes into effect at very light load operation.

$$V_{snubber} = \frac{1}{2} \left( \sqrt{V_{reflected}^2 + 2 \frac{L_{leakage} I_{pri}^2 R_{snubber}}{T_s}} - V_{reflected} \right)$$

$$P_{snubber} = \frac{(V_{snubber} + V_{reflected})^2}{R_{snubber}}$$

**Table 5**

Parameter	Symbol	600 V design	800 V P7 design
Leakage inductance	L <sub>leakage</sub>	25 μH	25 μH
Peak primary current under load at high line	I <sub>pri</sub>	0.43 A	0.48 A
Snubber resistor	R <sub>snubber</sub>	54 kΩ	300 kΩ
Switching period	T <sub>s</sub>	28.6 μs	28.6 μs
Snubber voltage	V <sub>snubber</sub>	40.1 V	127 V

Increasing the reflected voltage and lowering the amount of energy that is dissipated in the snubber lowers the overall system losses and would not be possible with a 600 V MOSFET as shown in Table 5. Even with increasing the reflected voltage by 94 V and increasing the snubber voltage by 30.4 V we still have an increase in margin from the MOSFET breakdown voltage. In this new design the margin has increased from 12% to 15% even with increasing the V<sub>DS</sub> voltages. This allows for the design of flyback converters running from higher input bus voltages or those that need margin for abnormal conditions such as surge.

**Table 6**

Parameter	Symbol	600 V design	800 V P7 design
Primary bus voltage @265 V <sub>AC</sub>	V <sub>bus</sub>	373 V	373 V
Reflected voltage	V <sub>reflected</sub>	117 V	211 V
Snubber voltage	V <sub>snubber</sub>	40.1 V	70.5 V
Drain source voltage maximum	V <sub>DS_max</sub>	526 V	622 V
Margin from breakdown voltage	V <sub>DS_margin</sub>	12 %	15 %

## 5.2 UVLO circuit

The Under Voltage Lock Out (UVLO) circuit provides a mechanism to shut down the power supply when the AC line input voltage is lower than the specified voltage range. The UVLO event is detected by sensing the voltage level at U2's (TL431) REF pin (V<sub>REF\_typ</sub> = 2.5 V) through the voltage divider resistors (R12, R13, R14, and R17 in Figure 12) from the bulk capacitor C1. Q2 acts as a switch to enter or leave UVLO mode by controlling the FB pin voltage. Q3, together with R17, acts as voltage hysteresis for the UVLO circuit and U2 (TL431) as a comparator. The system enters the UVLO mode by controlling the FB pin voltage of U1 to 0 V (when the voltage input level goes back to input voltage range), V<sub>REF</sub> increases to 2.5 V (then switches Q2 and Q3 off) and V<sub>CC</sub> hits 18 V, the UVLO mode is released. The calculation for the UVLO circuit is shown below:

$$V_{REF} = 2.5 \text{ V}$$

$$R12 = 4.99 \text{ M}\Omega \quad R13 = 4.99 \text{ M}\Omega \quad R14 = 330 \text{ k}\Omega \quad R17 = 681 \text{ k}\Omega$$

$$V_{bulk\_enterUVLO} = \frac{(R12 + R13 + R14)V_{ref}}{R14}$$

Design considerations

$$V_{bulk\_leaveUVLO} = \frac{\left[ \left( \frac{R14R17}{R14 + R17} \right) + R12 + R13 \right] V_{ref}}{\left( \frac{R14R17}{R14 + R17} \right)}$$

$$V_{bulk\_enterUVLO} = 77.8 V_{DC}$$

$$V_{bulk\_leaveUVLO} = 114.3 V_{DC}$$

The 'enter UVLO' threshold is set at  $77.8 V_{DC}$  to allow for the BUS capacitance voltage to droop under  $90 V_{AC}$  at full load operation with some margin to avoid false triggering.

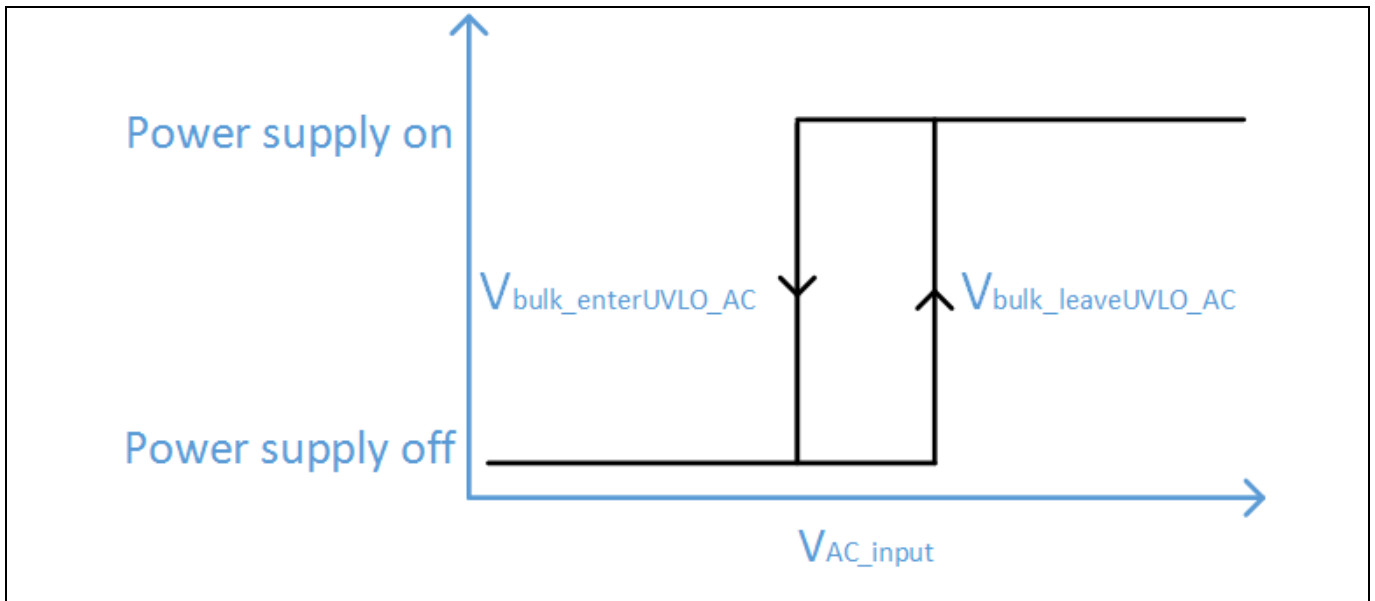


Figure 12 Power supply status vs. AC input voltage showing the hysteretic behavior of the UVLO circuit.

## 6 Demo board overview

### 6.1 Demo board pictures

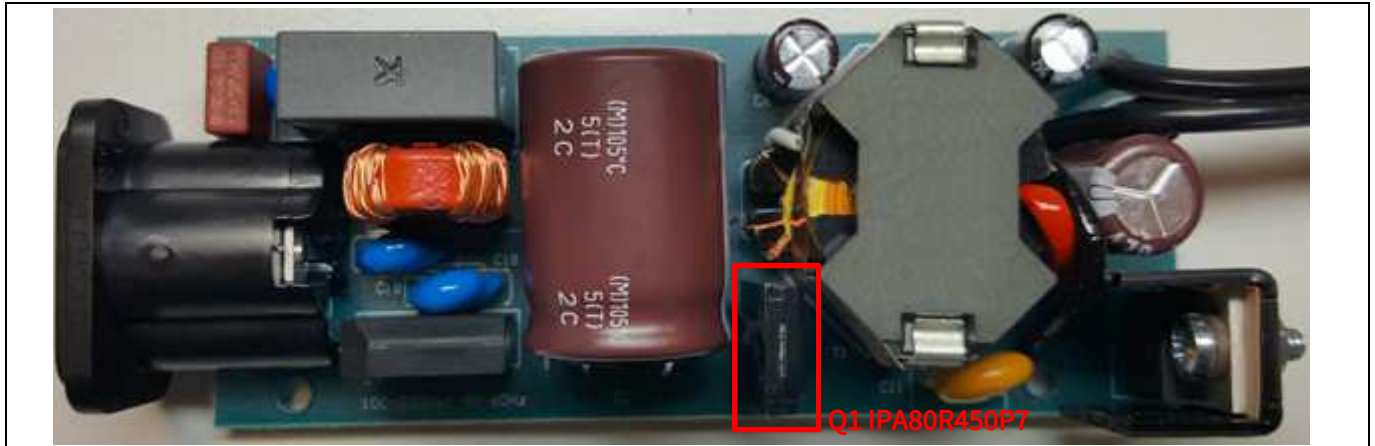


Figure 13 Top side of 45 W IFX adapter with a TO220 FullPAK populated

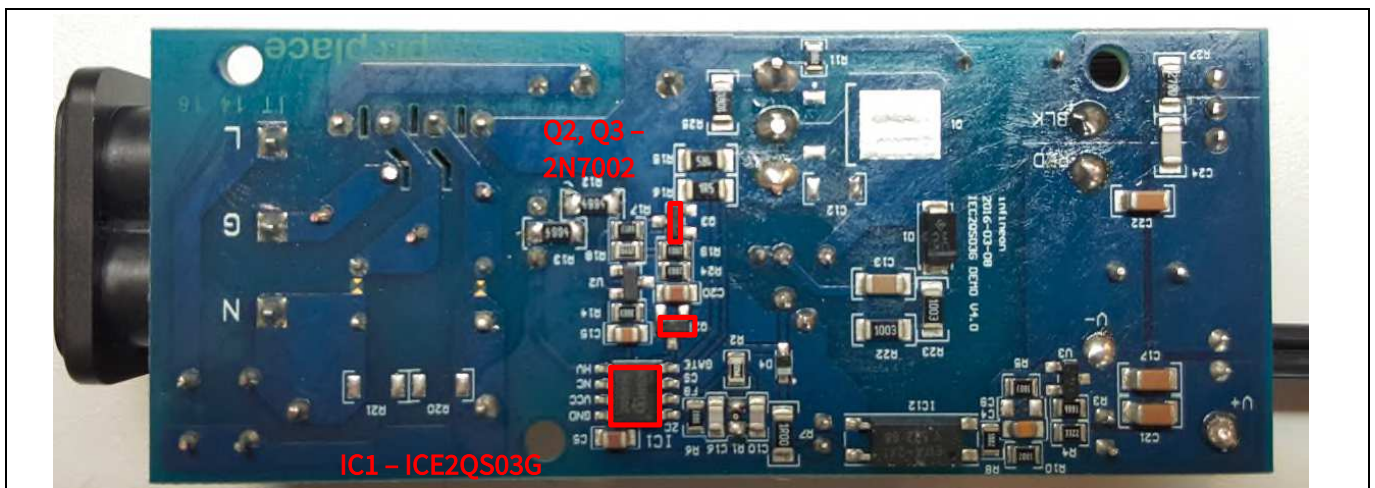


Figure 14 Bottom side of 45 W IFX adapter highlighting Infineon components. The Q1 DPAK is not populated on the bottom side since the board is populated with a FullPAK device.

### 6.2 Demo board specifications

Table 7

Section	Parameter	Specification
Input ratings	Input voltage	90 V <sub>AC</sub> – 265 V <sub>AC</sub>
	Input frequency	47 Hz – 63 Hz
	Input current at 100 V <sub>AC</sub> , 45 W	0.82 A maximum
	Power factor	0.55 @100 V <sub>AC</sub> 0.37 @265 V <sub>AC</sub>
	Peak efficiency 230 V <sub>AC</sub> , 45 W	91.4%
	Peak efficiency 120 V <sub>AC</sub> , 45 W	89.3%
	Surge	2 kV IEC61000-4-5

## Demo board overview

Section	Parameter	Specification
Output ratings	Nominal output voltage	19.0 V
	Tolerance	2%
	Output current	2.4 A
	Output power	45 W
	Line regulation	0.5%
	Load regulation	0.5%
	Output ripple	100 mV <sub>pp</sub>
	Quiescent power draw	42 mW @100 V <sub>AC</sub> 94 mW @265 V <sub>AC</sub>
	Switching frequency	25 – 60 kHz
	Mechanical	Dimensions
Width: 3.7 cm (1.46 in.)		
Height: 2.6 cm (1.02 in.)		
Environmental	Ambient operating temperature	-25°C to 50°C

### 6.3 Demo board features

- **Fold back point protection** - For a quasi-resonant flyback converter, the maximum possible output power is increased when a constant current limit value is used across the entire mains input voltage range. This is usually not desired as this will increase the cost of the transformer and output diode in the case of output over power conditions. The internal fold back protection is implemented to adjust the  $V_{CS}$  voltage limit according to the bus voltage. Here, the input line voltage is sensed using the current flowing out of the ZC pin, during the MOSFET on-time. As the result, the maximum current limit adjusts with the AC line voltage.
- **$V_{CC}$  over voltage and under voltage protection** - During normal operation, the  $V_{CC}$  voltage is continuously monitored. When the  $V_{CC}$  voltage increases to WCC OVP or  $V_{CC}$  voltage falls below the under voltage lock out level WCC off, the IC will enter into auto restart mode.
- **Over load/open loop protection** - In the case of an open control loop, the feedback voltage is pulled up with an internal block. After a fixed blanking time, the IC enters into auto restart mode. In case of a secondary short-circuit or overload, the regulation voltage  $V_{FB}$  will also be pulled up, the same protection is applied and the IC will auto restart.
- **Adjustable output overvoltage protection** - During the off-time of the power switch, the voltage at the zero-crossing pin, ZC, is monitored for output overvoltage detection. If the voltage is higher than the preset threshold 3.7 V for a preset period of 100  $\mu$ s, the IC is latched off.
- **Auto restart for over temperature protection** - The IC has a built-in over temperature protection function. When the controller's temperature reaches 140 °C, the IC will shut down the switch and enters into auto restart. This can protect the power MOSFET from overheating.
- **Short winding protection** - The source current of the MOSFET is sensed via external resistors, R15 and R16. If the voltage at the current sensing pin is higher than the preset threshold VCSSW of 1.68 V during the on-time of the power switch, the IC is latched off. This constitutes a short winding protection. To avoid an accidental latch off, a spike blanking time of 190 ns is integrated in the output of internal comparator.

### 6.4 Schematic

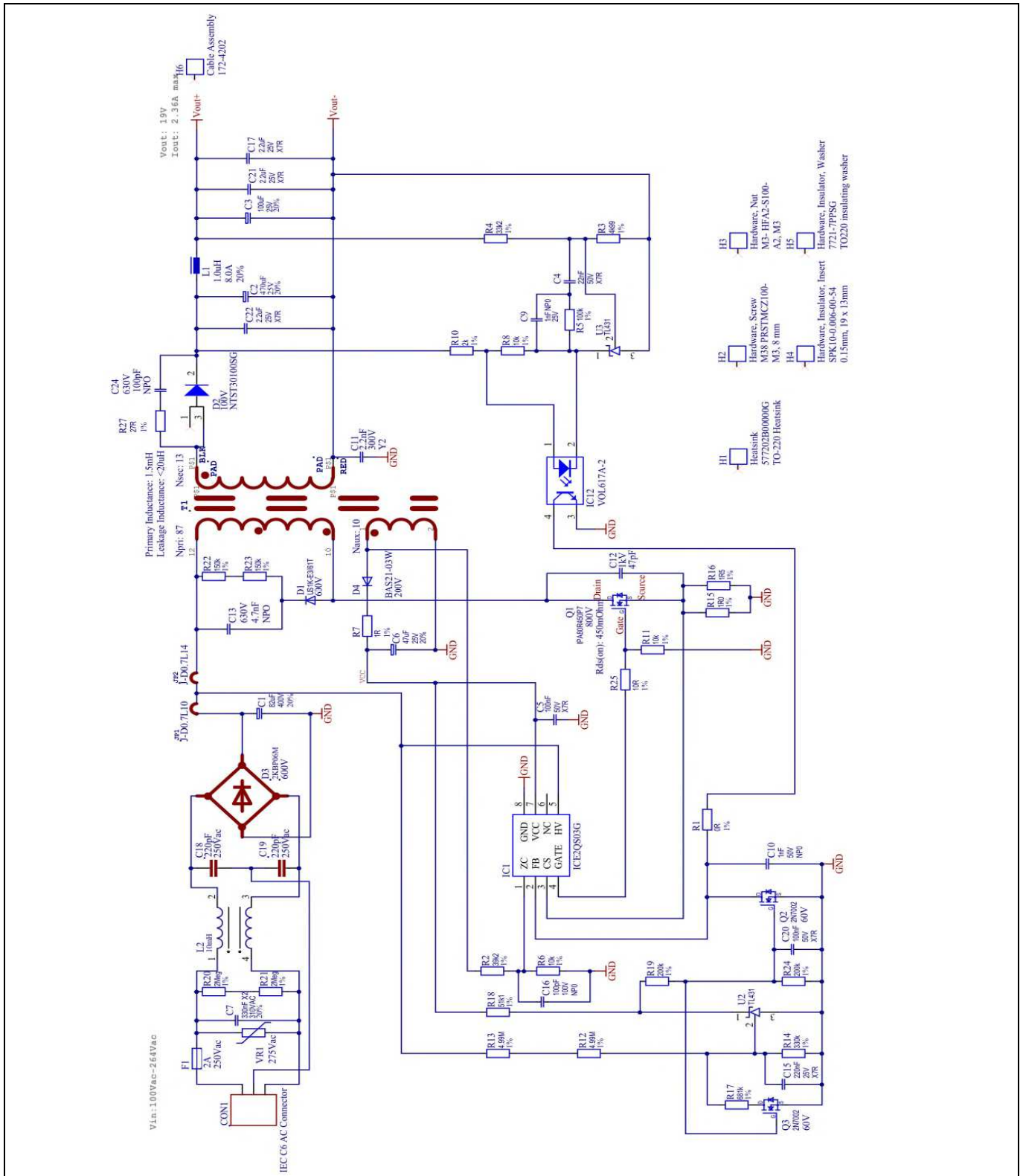


Figure 15 45 W adapter schematic

## 6.5 BOM with Infineon components in bold

Table 8

Reference	Description	Part number	Manufacturer
C1	Electrolytic capacitor, 82 uF, 20%, 400 V	EKXG401ELL820MM25S	United Chemi-Con
C2	Electrolytic capacitor, 470 uF, 20%, 25 V	EKZE250ELL471MJ16S	United Chemi-Con
C3	Electrolytic capacitor, 100 uF, 20%, 25 V	EEU-FR1E101	Panasonic
C4	Capacitor ceramic, 22 nF, X7R, 50 V, CAP0805W	VJ0805Y223KNAAO	Vishay
C5, C20	Capacitor ceramic, 100 nF, X7R, 50 V, CAP0805W	C2012X7R2A104K125AA	TDK
C6	C_ELKO, 47uF, 20%, 25V, C_Aluminium Elektrolyt 5 mm	UPM1E470MED	Nichicon
C7	Foil capacitor, 330 nF X2, 20%, 310 V <sub>AC</sub> , C_Foil 15 mm - V2	R463I33305002K	Kemet
C10	Capacitor ceramic, 1nF, NP0, 50 V, CAP0805W	CGA4C2C0G1H102J060AA	TDK
C11	Capacitor Y2, 2.2 nF, Y2, 300 V, CAP-DISC 7.5 mm	AY2222M35Y5US63L7	Vishay
C13	Capacitor ceramic, 4.7 nF, NPO, 630 V, CAP1206W	C1206C472JBGACTU	Kemet
C15	Capacitor ceramic, 220 nF, X7R, 25 V, CAP0805W	C2012X7R1H224K125AA	TDK
C16	Capacitor ceramic, 100pF, NP0, 100 V, CAP0805W	CGA4C2C0G2A101J060AA	TDK
C17, C21, C22	Capacitor ceramic, 2.2 uF, X7R, 25 V, CAP1206W	C3216X7R1E225K160AA	TDK
C18, C19	220pF/250 VAC, 220pF, 250 V <sub>ac</sub> , C075-045X100	VY2221K29Y5SS63V0	Vishay
C24	Capacitor ceramic, 100 pF, NPO, 630 V, CAP1206W	CGA5C4C0G2J101J060AA	TDK
CON1	ST-04A, IEC C6 AC Connector, ST-A04	6160.0003	Schurter
D1	Diode, US1K-E3/61T, 600V, SMA	US1K-E3/61T	Vishay
D2	Diode, NTST30100SG, 100V, TO220_standing	NTST30100SG	OnSemi
D3	2KBP06M, 2KBP06M, 600V, KBPM	2KBP06M-E4/51	Vishay
D4	Diode, BAS21-03W, 200V, SOD323	BAS21HT1G	OnSemi
F1	T2, 2 A, 250 V <sub>ac</sub> , Fuse small	40012000440	Littelfuse
H1	Heatsink, TO-220 Heatsink	577202B00000G	Aavid thermalloy
H2	Hardware, Screw, M3, 8 mm	M38 PRSTMCZ100-	DURATOOL
H3	Hardware, Nut, A2, M3	M3- HFA2-S100-	DURATOOL
H4	Hardware, insulator, Insert, 0.15 mm, 19 x 13 mm	SPK10-0.006-00-54	Bergquist
H5	Hardware, insulator, washer, TO220 insulating washer	7721-7PPSG	AAVID THERMALLOY



Demo board overview

Reference	Description	Part number	Manufacturer
H6	Cable assembly	172-4202	Memory Protection Devices, Inc.
IC1	QR PWM controller	ICE2QS03G	Infineon
IC12	VOL617A-2, VOL617A-2, LSOP 4pin	VOL617A-2X001T	Vishay
L1	Choke, 1.0 uH, 20%, INDUCTOR 4 u7 4,2 A	7447462010	Würth
L2	Inductance, 10 mH, Inductor common mode small	744821110	Würth
Q1	NMOS, IPA80R450P7, 800V, TO220FP	IPA80R450P7	Infineon
Q2, Q3	NMOS, 2N7002, 60V, SOT23	2N7002	Infineon
R1	Resistor, 0R, 1%, RES0805R	CRCW08050000Z0EA	Vishay
R2	Resistor, 39k2, 1%, RES0805R	ERJ6ENF3922V	Panasonic
R3	Resistor, 4k99, 1%, RES0805R	CRCW08054K99FKEA	Vishay
R4	Resistor, 33k2, 1%, RES0805R	CRCW080533K2FKEA	Vishay
R5	Resistor, 100k, 1%, RES0805R	CRCW0805100KFKEA	Vishay
R6, R8, R11	Resistor, 10k, 1%, RES0805R	CRCW080510K0FKEA	Vishay
R15, R7	Resistor, 1R, 1%, RES1206W	CRCW12061R00FKEA	Vishay
R10	Resistor, 2k, 1%, RES0805R	CRCW08052K00FKEA	Vishay
R12, R13	Resistor, 4.99M, 1%, RES1206W	CRCW12064M99FKEB	Vishay
R14	Resistor, 330k, 1%, RES0805R	CRCW0805330KFKEA	Vishay
R16	Resistor, 1R5, 1%, RES1206W	CRCW12061R50JNEAIF	Vishay
R17	Resistor, 681k, 1%, RES0805R	CRCW0805681KFKEA	Vishay
R18	Resistor, 51k1, 1%, RES0805R	ERJ6ENF5112V	Panasonic
R19, R24	Resistor, 200k, 1%, RES0805R	CRCW0805200KFKEA	Vishay
R22, R23	Resistor, 150k, 1%, RES1206W	CRCW1206150KFKEA	Vishay
R25	Resistor, 10R, 1%, RES1206W	CRCW120610R0FKEA	Vishay
R27	Resistor, 27R, 1%, RES1206W	CRCW120627R0FKEA	Vishay

6.6 PCB layout

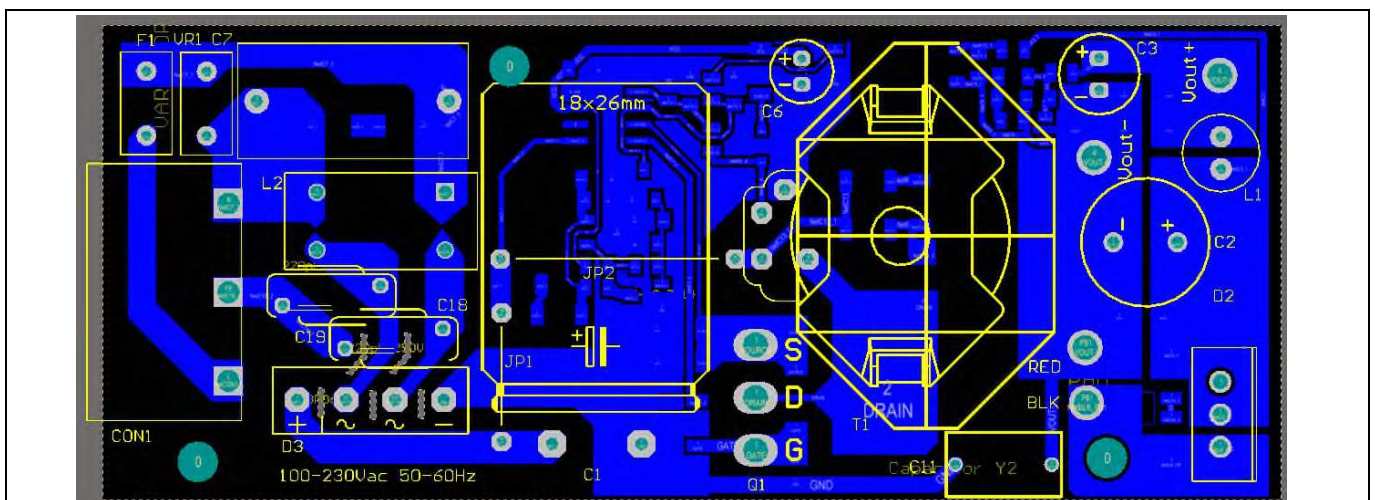


Figure 16 Board layout top

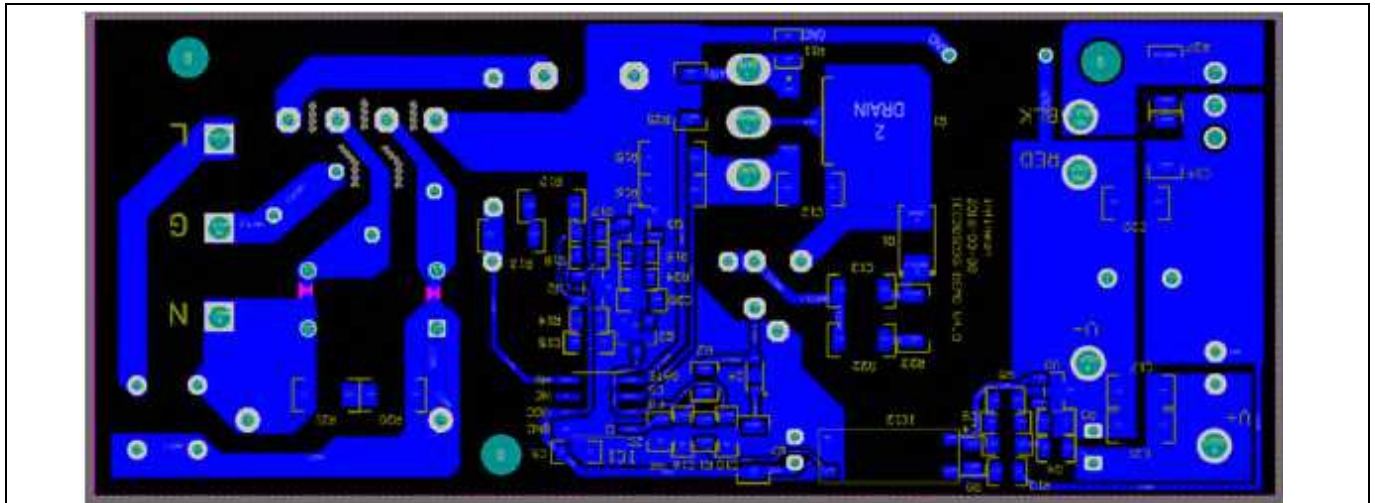


Figure 17 Board layout bottom

The PCB was designed using Altium Designer 16. Schematic and board files are available on request.

### 6.7 Transformer construction

The transformer for the 45 W adapter was built by I.C.E. Transformers: <http://www.icetransformers.com/>

Table 9 Transformer specification

Manufacturer	I.C.E. Transformers
Core size	RM10
Core material	3C95
Bobbin	8 pin RM10 vertical
Primary inductance	1500 $\mu$ H measured from pin 1 to pin 3 @10 kHz
Leakage inductance	< 25 $\mu$ H measured from pin 1 to pin 3 with all other pins shorted @10 kHz

\*100% of components are Hi-Pot tested to 4.2 kV primary to secondary for 1 minute

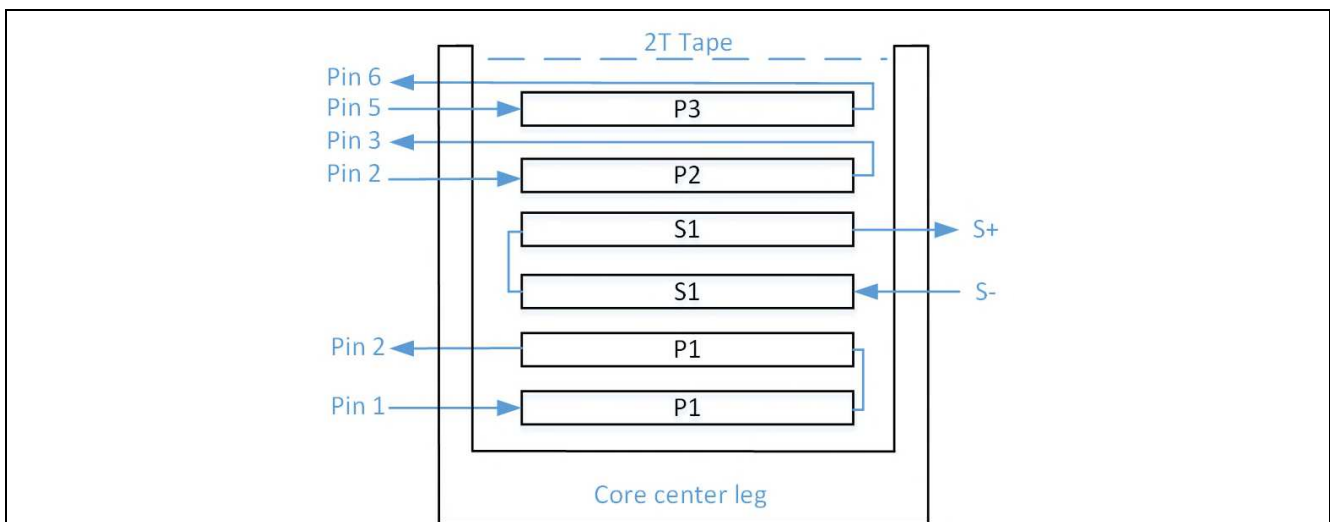


Figure 18 Transformer windings stackup

## 45 W adapter demo board

### Using the new 800 V CoolMOS™ P7 and ICE2QS03G quasi-resonant PWM controller



#### Demo board overview

1. S- in red tube, S+ in black tube
2. S- length 25 mm, solder length 5 mm
3. S+ length 30 mm, solder length 5 mm
4. Cut pin 4, pin 2, core clip PCB mount pins, and secondary pins.
5. Add a flux band of 8mm copper foil with 2 layers of tape and 3mm of cuffing on each side. Add around the core with the tape side facing out. Using  $\phi 0.35$  mm solder to pin 5.
6. Vacuum varnish the entire assembly.
7. Cut off core clamp pins

**Table 10** Transformer windings stackup

Name	Start	Stop	Turns	Wire	Layer	Method
P1	1	2	58	1 x $\phi 0.35$ mm	primary	tight
S1	S-	S+	13	2 x $\phi 0.5$ mm triple insulated	secondary	tight
P2	2	3	29	1 x $\phi 0.35$ mm	primary	tight
P3	5	6	10	1 x $\phi 0.15$ mm, with margin tape	auxiliary	evenly spaced
T1			2	tape		

## 7 Measurements

### 7.1 Test measurements under different line and load conditions

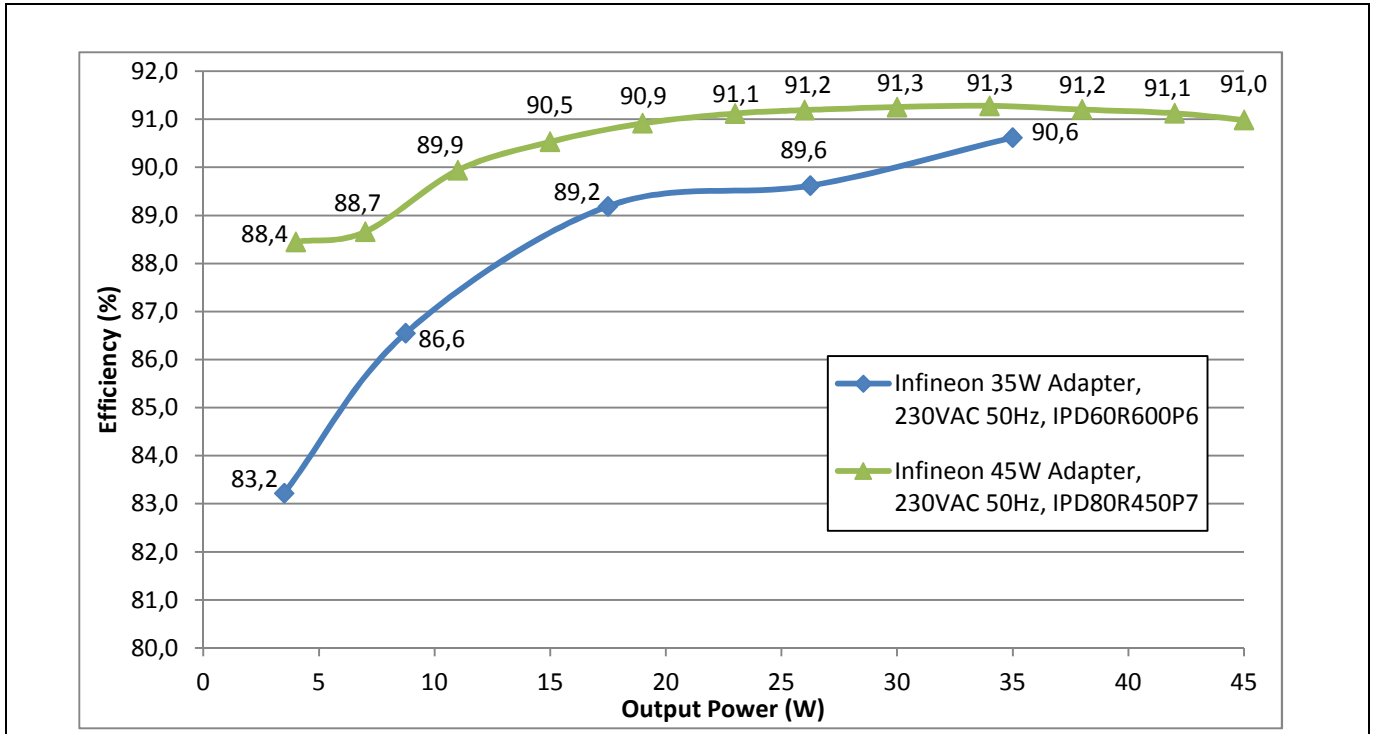


Figure 19 45 W adapter efficiency at 230 V<sub>AC</sub> using IPA80R450P7 when compared to Infineon 35 W adapter using IPD60R600P6

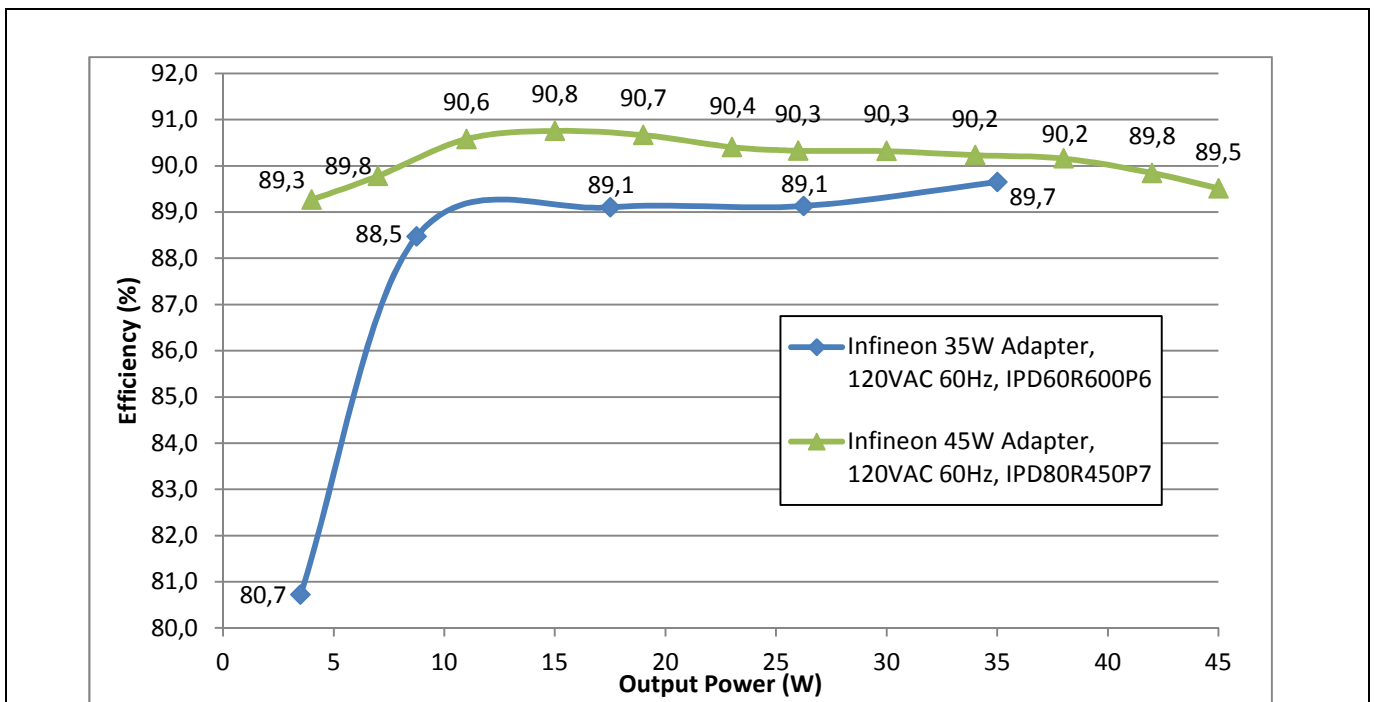


Figure 20 45 W Adapter efficiency at 120 V<sub>AC</sub> using IPA80R450P7 when compared to Infineon 35 W adapter using IPD60R600P6

## 7.2 Normal operation

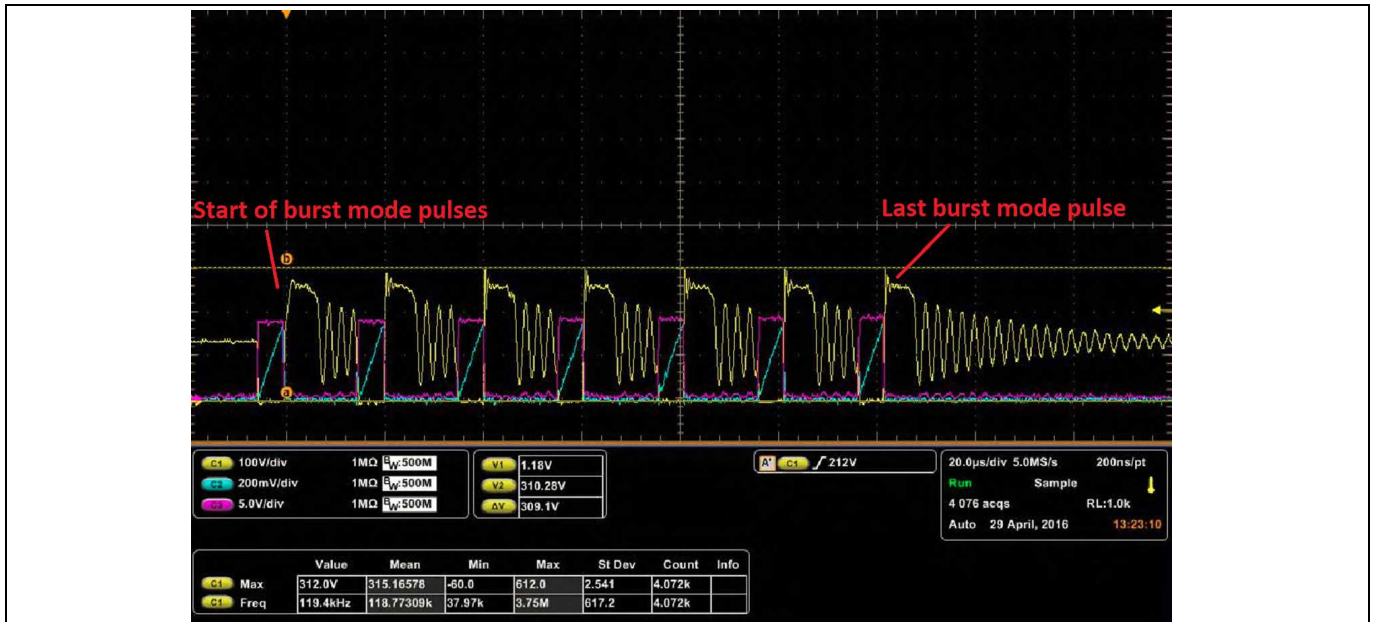


Figure 21 Low line (100 V<sub>AC</sub>), no load, The ICE2QS03G is operating in burst mode to minimize the idle power consumption. The burst mode pulse train shown above occurs every 33.8 ms with the main switch inactive in the period between pulse trains to lower light load power consumption.

- CH1 (Yellow): Q1 V<sub>DS</sub>
- CH2 (Cyan): Q1 I<sub>DS</sub>
- CH3 (Magenta): Q1 V<sub>GS</sub>

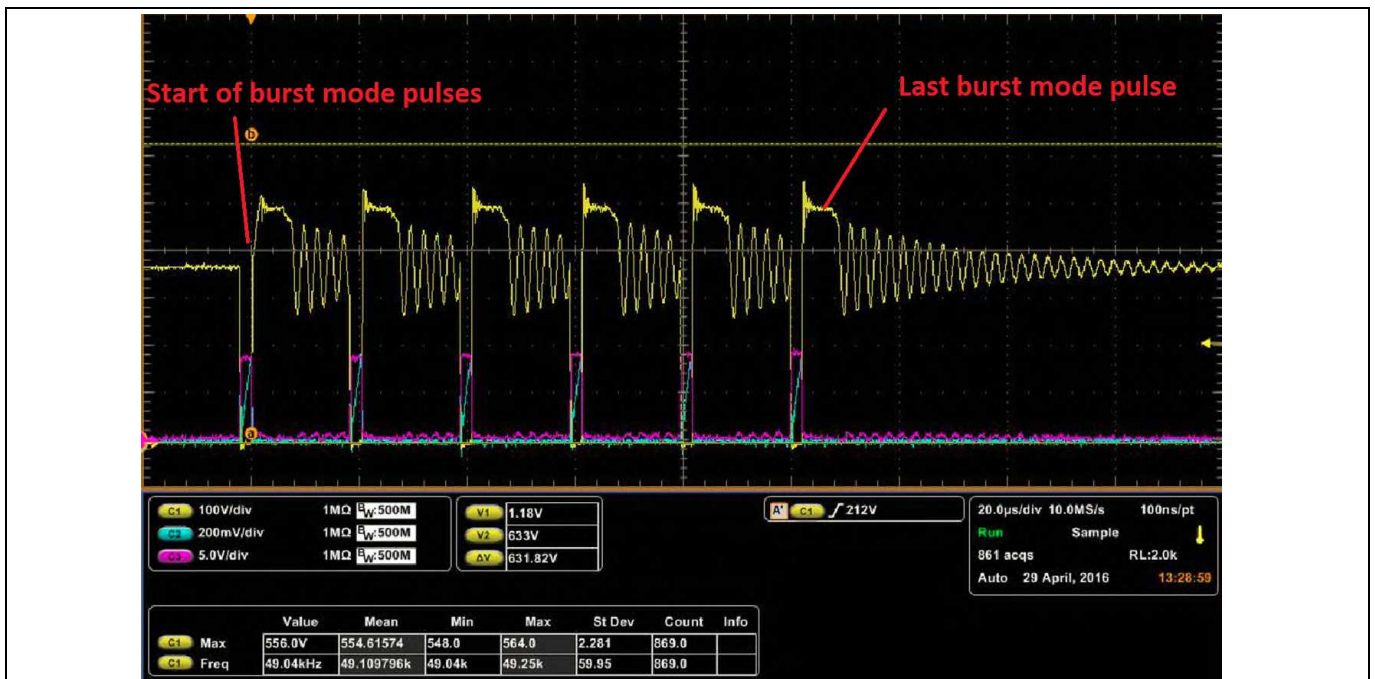


Figure 22 High line (265 V<sub>AC</sub>), no load, The ICE2QS03G is operating in burst mode to minimize idle power consumption. The burst mode pulse train shown above occurs every 33.8 ms.

- CH1 (Yellow): Q1 V<sub>DS</sub>
- CH2 (Cyan): Q1 I<sub>DS</sub>
- CH3 (Magenta): Q1 V<sub>GS</sub>

Measurements

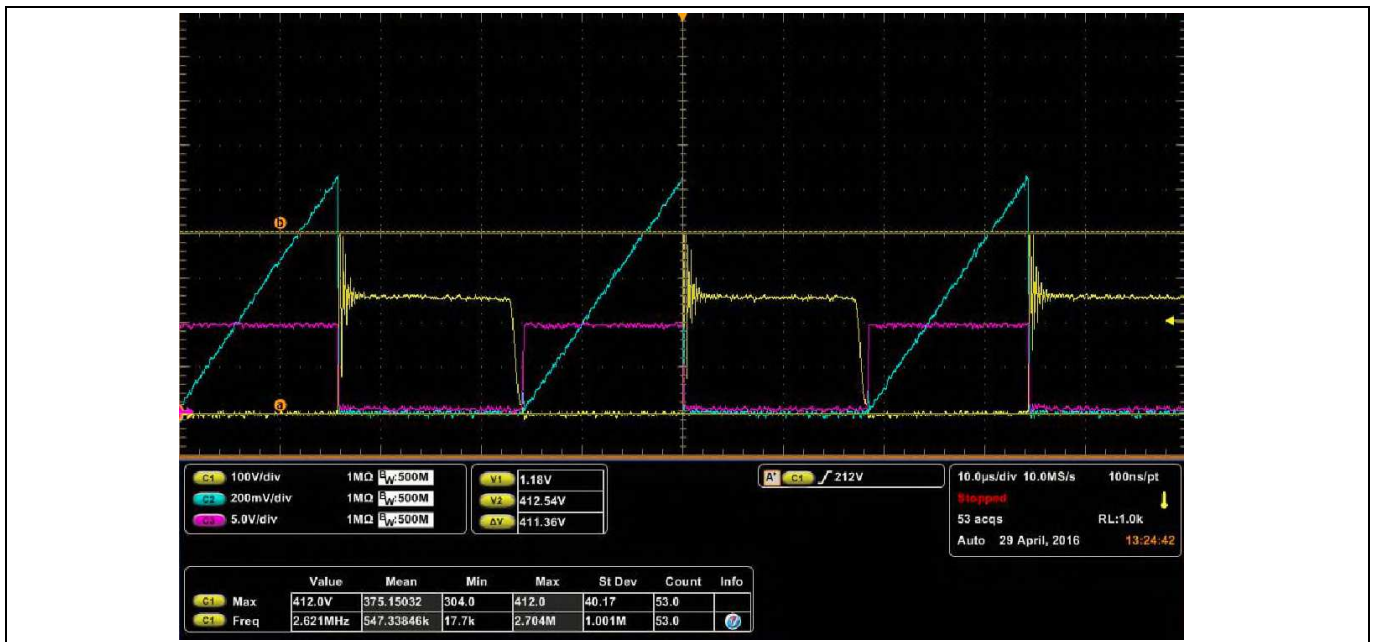


Figure 23 Low line (100V<sub>AC</sub>), Full load (45 W) showing normal full load operation of the adapter. This is the worst case peak current that the primary MOSFET Q1 will encounter during normal operation.

CH1 (Yellow): Q1 V<sub>DS</sub>

CH2 (Cyan): Q1 I<sub>DS</sub>

CH3 (Magenta): Q1 V<sub>GS</sub>

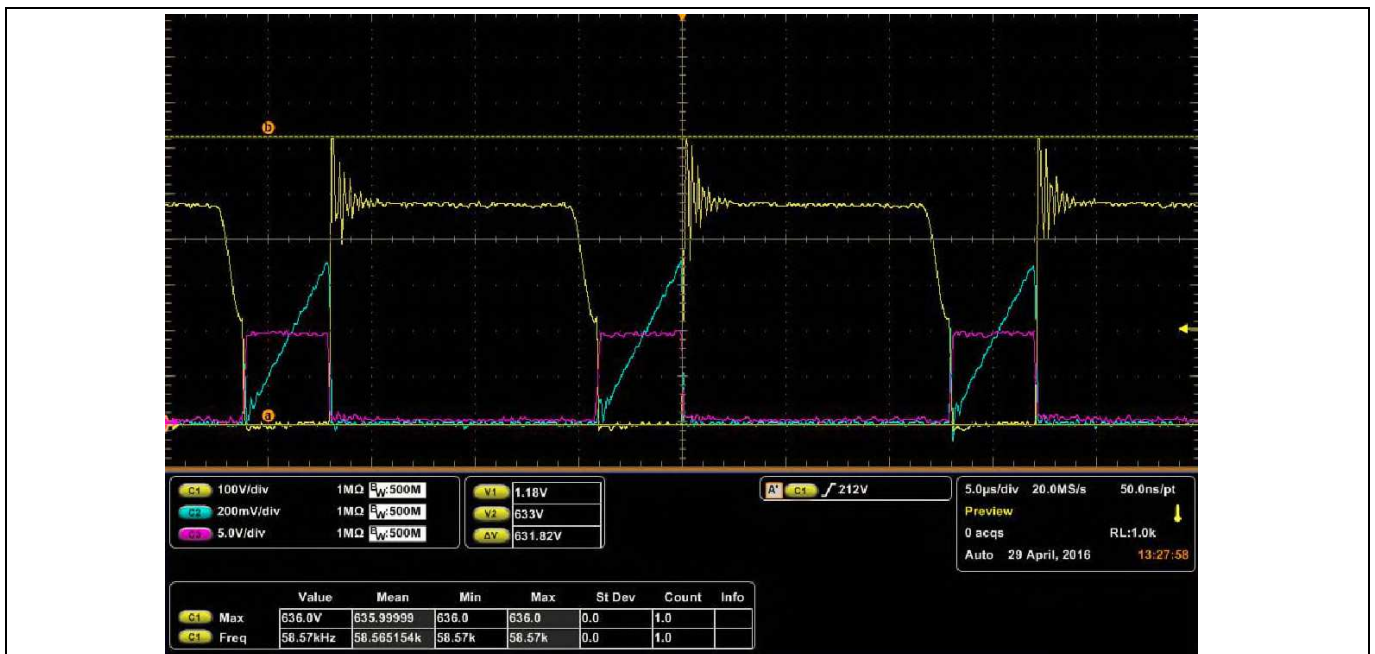


Figure 24 High line (265 V<sub>AC</sub>), Full load (45 W) showing normal full load operation of the adapter. This is the worst case peak drain source voltage that the MOSFET will see under normal operating conditions.

CH1 (Yellow): Q1 V<sub>DS</sub>

CH2 (Cyan): Q1 I<sub>DS</sub>

CH3 (Magenta): Q1 V<sub>GS</sub>

### 7.3 Surge testing

In order for the power supply to be robust enough for abnormal line conditions such as lightning strikes or failures of other electronics on the line, it needs to survive surge testing. The 45 W power supply was tested to the 2 kV EN61000 surge conditions and still had 96 V of margin under worst case conditions for the MOSFET  $V_{DS}$ .

**Table 11** EN61000 surge requirements

Level	Surge voltage L-N (kV)	Surge voltage L-PE, N-PE (kV)
Class 1 protected environment	0.25	0.5
Class 2 electrical cables are separated	0.5	1.0
<b>Class 3 electrical cables run in parallel</b>	<b>1.0</b>	<b>2.0</b>
Class 4 outdoor	2.0	4.0

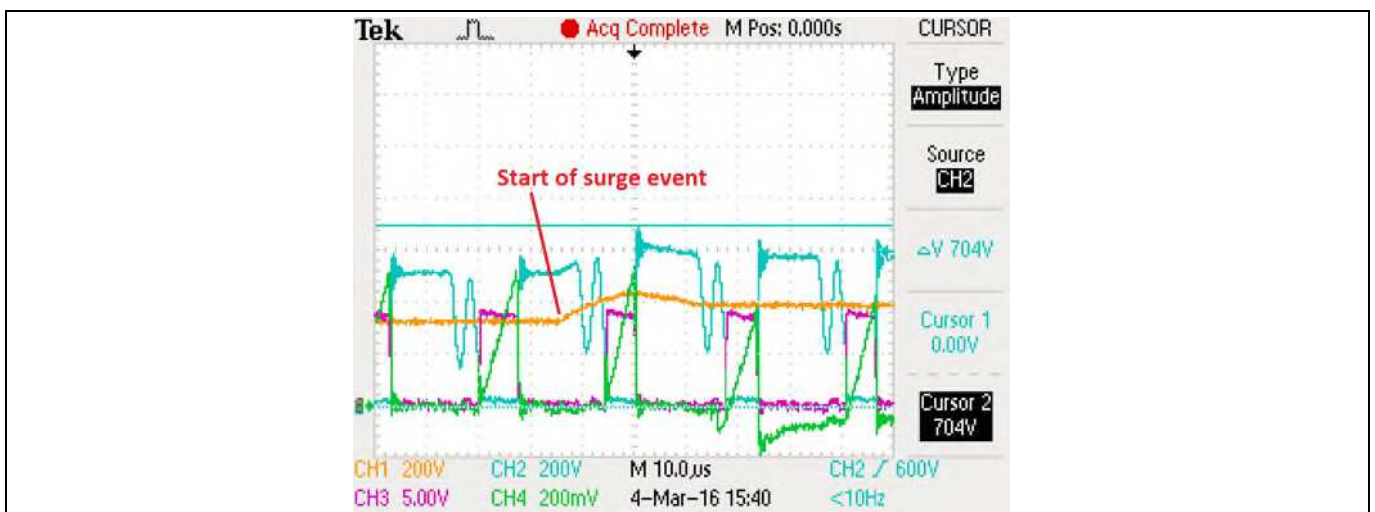


**Figure 25** IEC61000 2 kV surge test was performed on the adapter while operating under full load (45 W). The highest voltage that was reached across the Q1  $V_{DS}$  was 704 V. The surge event can be seen on CH1 when the  $V_{BUS}$  rapidly rises. The bus capacitor (C1) and line filter values are critical for determining the peak surge voltage.

- CH1 (Yellow):  $V_{C1}, V_{BUS}$
- CH2 (Cyan):  $Q1 V_{DS}$
- CH3 (Magenta):  $Q1 V_{GS}$
- CH4 (Green):  $Q1 I_{DS}$

### 7.4 Thermal performance under typical operating conditions

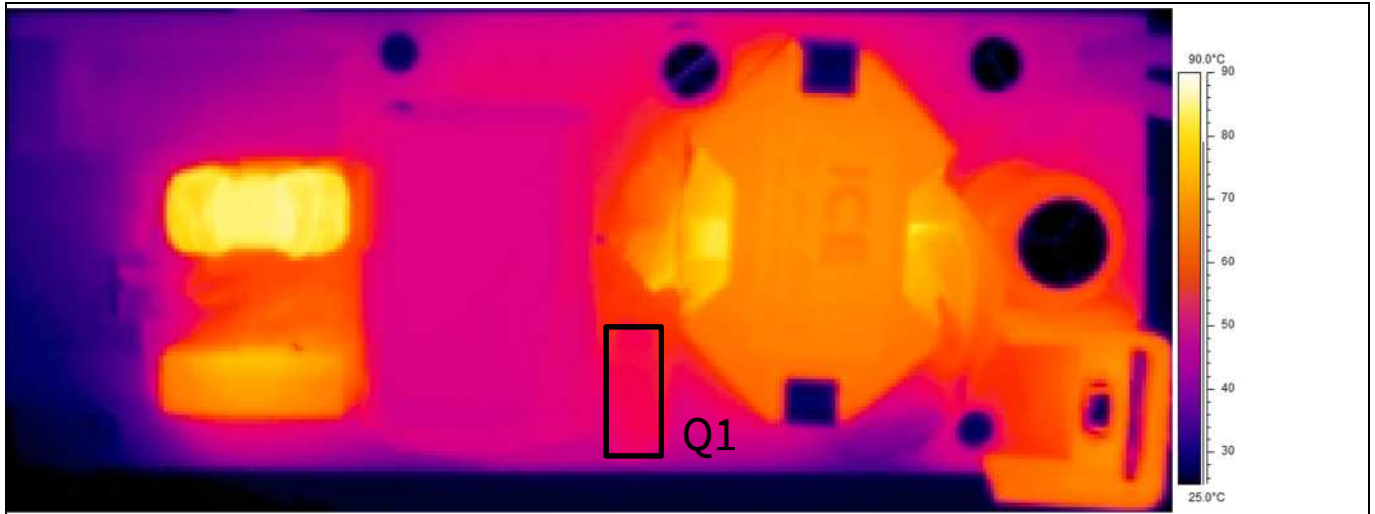


Figure 26 100 V<sub>AC</sub> input, full load, top side. The line filter and bridge rectifier are hottest at this point due to higher AC input currents.

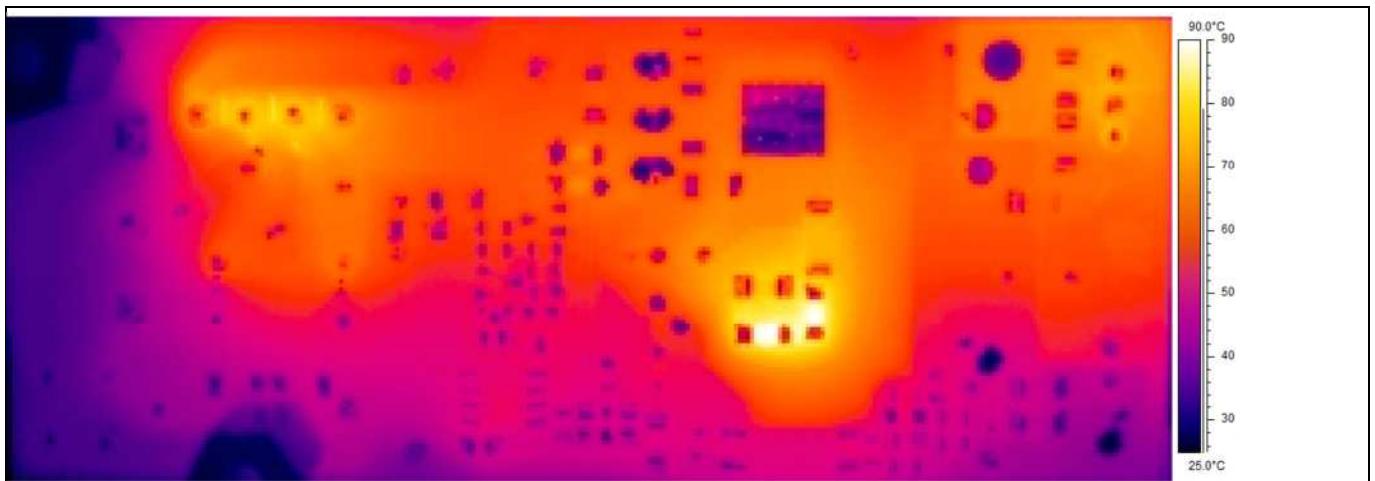


Figure 27 100 V<sub>AC</sub> input, full load, bottom side.

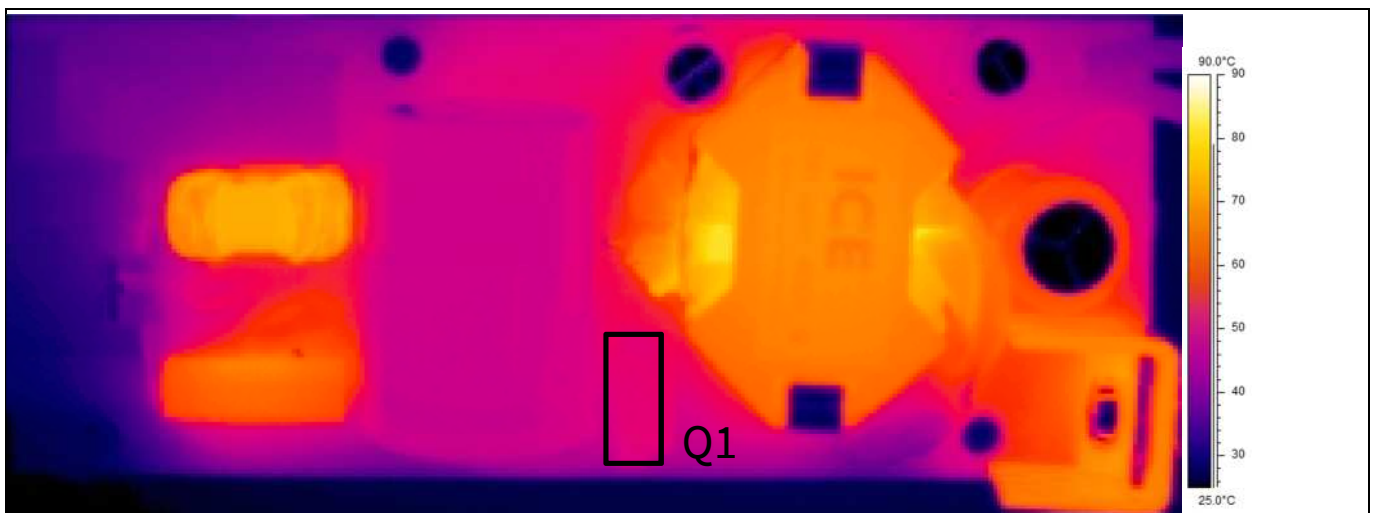


Figure 28 120 V<sub>AC</sub> input, full load, top side. The line filter and bridge rectifier are hotter at this point due to the higher primary side current.



Measurements

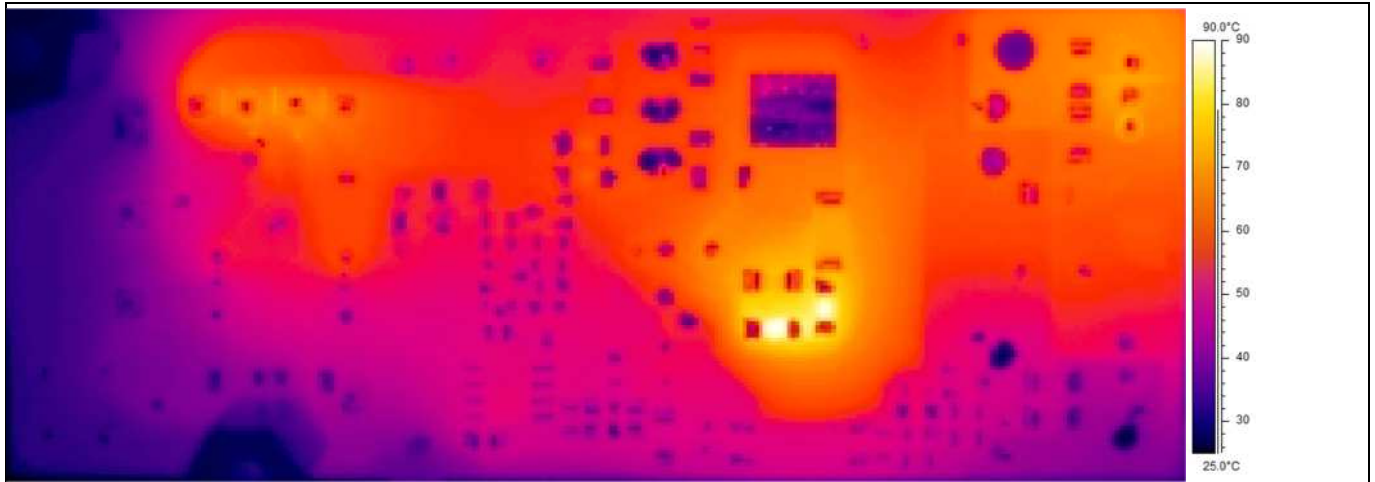


Figure 29 120 V<sub>AC</sub> input, full load, bottom side.

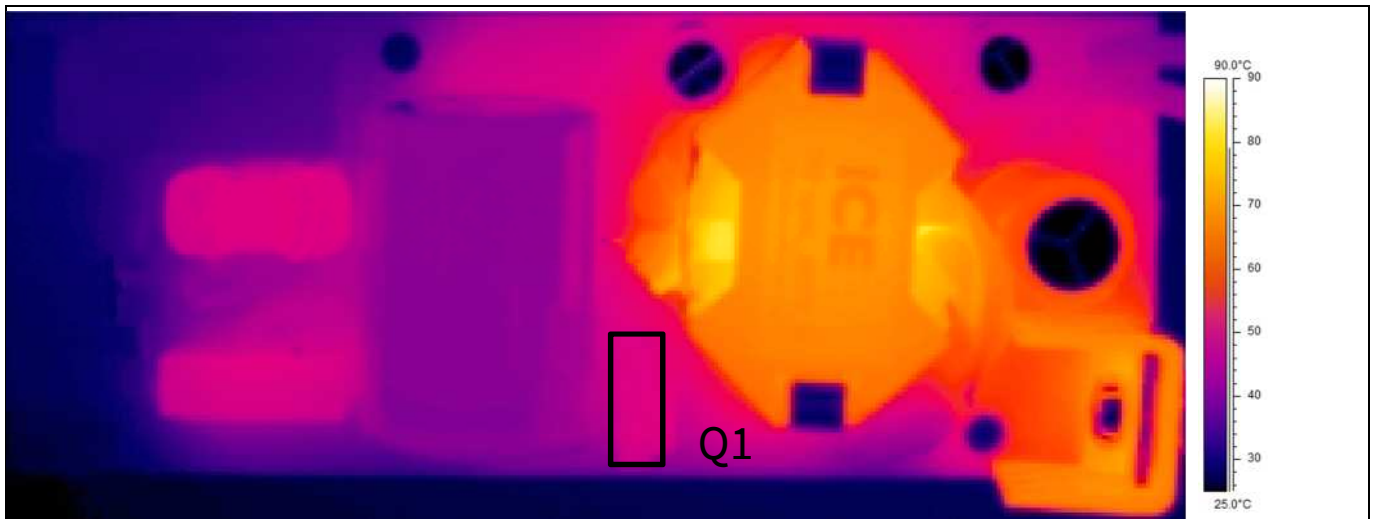


Figure 30 230 V<sub>AC</sub> input, full load, top side. The primary MOSFET (Q1) is cooler at 230 V<sub>AC</sub> because conduction losses become less dominant with lower primary side peak currents.

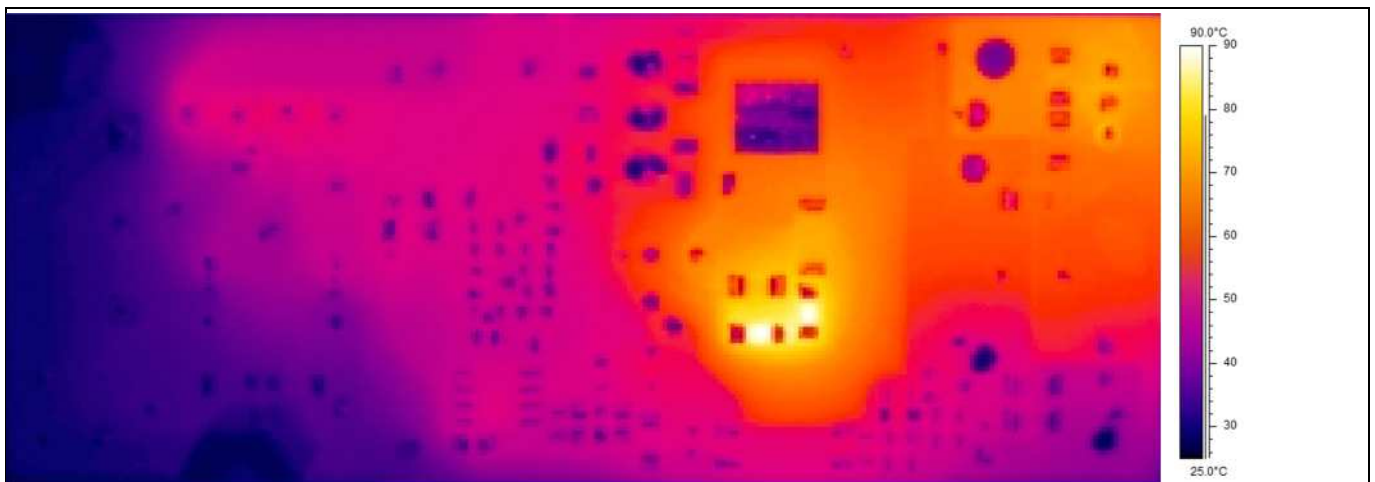


Figure 31 230 V<sub>AC</sub> input, full load, bottom side.

Measurements

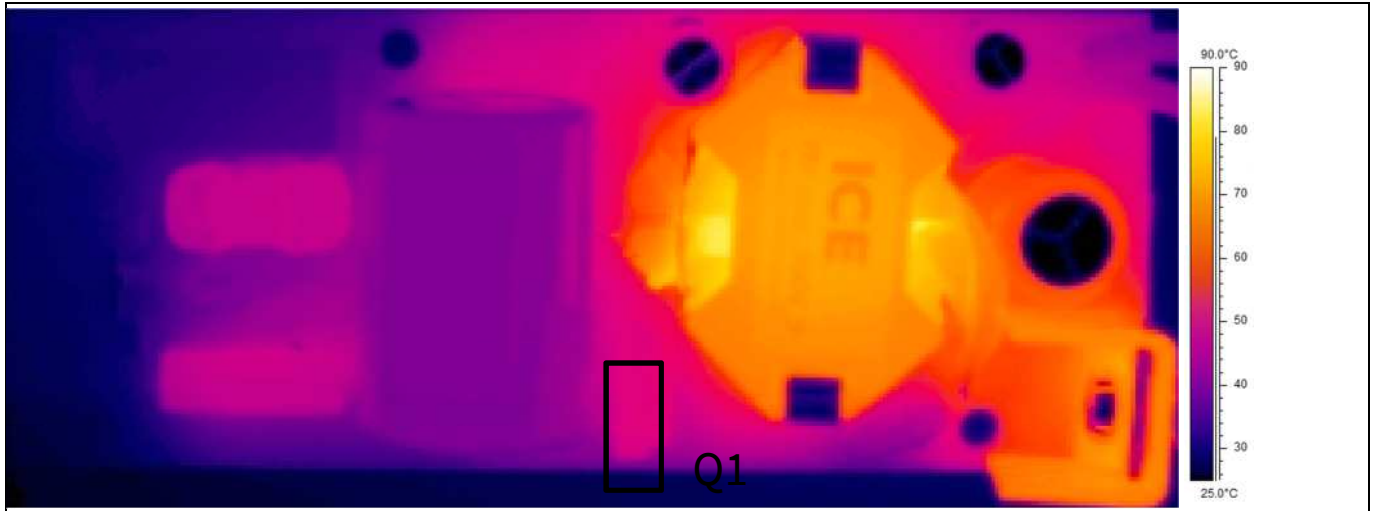


Figure 32 265 V<sub>AC</sub> input, full load, top side. The MOSFET is cooler at 230 V<sub>AC</sub> because conduction losses become less dominant with the lower primary peak currents.

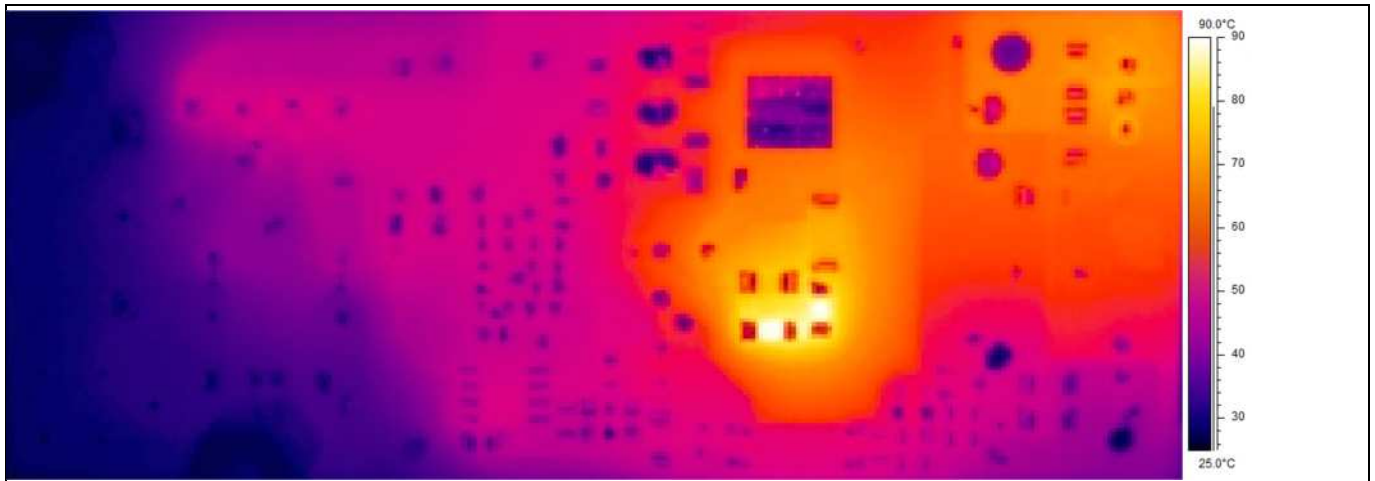


Figure 33 265 V<sub>AC</sub> input, full load, bottom side.